Experimental investigation of linear mode conversion in laser-produced plasmas

EXPERIMENTAL INVESTIGATION OF LINEAR MODE CONVERSION IN LASER-PRODUCED PLASMAS

PROEFSCHRIFT

ter verkrijging van de graad van doctor in de technische wetenschappen aan de Technische Hogeschool Eindhoven, op gezag van de rector magnificus, prof.ir. J.Erkelens, voor een commissie aangewezen door het college van dekanen in het openbaar te verdedigen op vrijdag 12 december 1980 te 16.00 uur

door

Alphonsus Gerardus Maria Maaswinkel

geboren te Roosendaal

DIT PROEFSCHRIFT IS GOEDGEKEURD
DOOR DE PROMOTOREN

Prof.dr. L.H.Th. Rietjens
en
Prof.dr. K.L. Kompa

voor mijn ouders

This work was supported by the Bundesministerium
für Forschung und Technologie and Euratom.

SUMMARY

"EXPERIMENTAL INVESTIGATION OF LINEAR MODE CONVERSION IN LASER-PRODUCED PLASMAS"

In this work absorption mechanisms are investigated in hot dense plasmas produced by intense laser irradiation of planar targets. Central in this investigation stands the absorption by linear mode conversion; this process occurs in inhomogeneous plasmas if the electric field vector of the incident EM-wave has a component parallel to the density gradient; this causes electrostatic oscillations at the critical density (where $\omega_{pe} = \omega$). In addition absorption of the laser light by inverse bremsstrahlung is investigated.

The absorption is determined by the reflection of the laser light from the plasma. To this aim optical diagnostics are used. The reflection into 4π sr is measured with an Ulbricht sphere, also the reflection in specular (geometric) direction is recorded. The absorption mechanisms have been isolated by variation of the polarization of the beam and the angle of incidence to the target.

An essential part of the work has been the frequency up-conversion of the laser beam by nonlinear crystals; in this way the wavelength-dependence of the absorption in the plasma has been investigated at wavelengths 1.06 μm, 0.53 μm and 0.26 μm; the pulse duration in the experiments was 30 ps, the maximum irradiation on target was 10^{14} W/cm^2.

A comparison of the experimental results with linear absorption mechanisms shows that the absorption is well described by linear mode conversion and inverse bremsstrahlung. From this it is concluded that lasers with short wavelengths ($\lesssim 0.3$ μm) and pulse duration of some ns are suitable candidates for larger systems in a laser-fusion reactor.

CONTENTS

V. DISCUSSION

I. GENERAL INTRODUCTION

Since the beginning of the 1960's, when the first proposals were made for heating small volumes of plasma to high temperatures using laser radiation /1/ there has been a continuously growing effort of producing hot dense plasmas by the impact of short giant laser pulses on solid targets. This interest was stimulated greatly in 1972, when it was first discussed in public that lasers with some kJ energy and pulse duration of 10 - 20 ns might be able to ignite a solid DT pellet by a suitable (isentropic) compression /2/.

One of the basic problems which have to be solved in order to achieve an effective compression and heating of the pellet is the absorption of the laser light by the target. Although in the past many experiments have been performed where the absorption from solid targets was investigated, there has been a considerable confusion between the results of these experiments. This was partially due to imperfections in the laser systems (spatially and temporally irreproducable pulse forms, focusing conditions). For another part it was caused by lack of suitable diagnostics, with which the amount of reflected and scattered laser light could be measured in an unambiguous way. This situation improved in 1977, when for the first time several groups /3, 4/ reported on measurements of the total reflectance of the plasma, recorded with reliable integrating detectors: in this way direct evidence of absorption by linear mode conversion was obtained. Still we are confronted with a situation where despite an abundance of experimental data the understanding of the absorption process is poor. In particular the dependence of the absorption on the wavelength and intensity of the laser has not been investigated.

For moderate laser intensities ($\leqslant 10^{14}$ W/cm^2) it is expected from theory that there are two linear absorption mechanisms which determine the absorption in the plasma.

First we mention the linear mode conversion, also called resonance absorption, which has the important property that it can absorb up to 50 % of the incident laser light, independent from the wavelength of the laser and independent of its intensity. It will be clear that verification of this theory in experiments is important with respect to large laser systems for fusion purposes, since it states that one may apply both short - as long wavelength lasers and irradiate with low or high intensities. The second mechanism is called inverse bremsstrahlung or collisional absorption. The theory for this process predicts that it is most effective if the laser light can penetrate deep into the plasma and if the electron temperature of the plasma is not too high. This implies that inverse bremsstrahlung should occur favourably in plasmas produced with short wavelength lasers.

In this thesis we have made an effort to perform a series of experiments on laser light absorption in order to compare the results with the theory. We have concentrated on the investigation of the primary absorption process under well defined conditions. For this purpose we have measured the reflectance from planar solid targets upon irradiation with a Nd/YAG laser with short (30 ps) pulses and a focal spot diameter of 40 - 60 μm. The maximum irradiation level thus obtained is 3.10^{14} W/cm^2; this is a relevant parameter, since the estimated irradiance on target in a laser fusion reactor is 10^{14} - 10^{15} W/cm^2. Within the short pulse duration the plasma expands over a distance of only 1 - 5 μm, which is small compared with the focal spot. Thus we approximate a plane geometry, which facilitates comparison of the data with the theory of absorption processes. In addition the steep plasma profile makes excitation of nonlinear absorption / reflection mechanisms improbable. To investigate the wavelength-dependence of the absorption mechanisms we have doubled and quadrupled the 1.06 μm laser light in frequency by nonlinear crystals; the efficiency of frequency doubling is about 30 %. In this way we have obtained absorption factors for wavelengths 1.06 μm, 0.53 μm and 0.26 μm.

We remark that the process of compression of solid matter by laser irradiation is very complex, and that many aspects of this process are not yet well understood: the absorbed energy has to be transported to the interior of the pellet, another problem is the hydrodynamic stability of the pellet. These are important problems which need detailed investigation in order to understand the physics behind them. They are, however, beyond the scope of this work, which deals with the primary absorption processes.

In the present work we give in chapter II a survey over the absorption process in laser-produced plasmas. An expression for collisional absorption is derived following the method described in /5, 6/; as an extension of the theory we compute the absorption for laser light obliquely incident on the target for different density profiles. Linear mode conversion is briefly discussed on the basis of a simple model. The role of instabilities is mentioned.

Chapter III describes the apparatus which we have used in the experiments (laser, crystals, diagnostics).

Chapter IV contains the experimental results, and consists of four publications. The first paper (§ 4.1) gives the results of the measurements made at wavelengths 1.06 μm and 0.53 μm at intensity 10^{14} W/cm^2. Collisional absorption and resonance absorption are demonstrated. The paper in § 4.2 describes the behaviour of the plasma upon irradiation at wavelength 0.26 μm and intensity 4×10^{13} W/cm^2. Here most absorption is by inverse bremsstrahlung, in addition resonance absorption is isolated. The third paper (§ 4.3) describes the radiation of the plasma at twice the laser frequency, which accompagnies linear mode conversion, and gives an independent confirmation of the theory. A particularly interesting feature predicted by the theory of linear mode conversion, namely its dependence on the density gradient of the plasma has been confirmed in the last

letter (§4.4). To this aim we have investigated resonance absorption in a weak probe beam of wavelength 1.06 μm by measuring the reflectance from a plasma produced with an intense 0.53 μm laser pulse. By delaying the probe pulse with respect to the main pulse the effect of the changing density profile on the absorption is demonstrated.

In chapter V finally the experimental results are discussed in relation to the theory described in chapter II.

References of chapter I:

1. N.G. Basov and O.N. Krokhin, Sov. Phys. JETP 19, 123 (1964)

2. J. Nuckolls, L. Wood, A. Thiessen, and G. Zimmerman, Nature 239, 139 (1972)

3. K.R. Manes, V.C. Rupert, J.M. Auerbach, P. Lee, and J.E. Swain, Phys. Rev. Lett. 39, 281 (1977)

4. R.P. Godwin, P. Sachsenmaier, and R. Sigel, Phys. Rev. Lett. 39, 1198 (1977)

5. V.L. Ginzburg, The Propagation of Electromagnetic Waves in Plasmas (Pergamon, Oxford, 1970)

6. P. Mulser and C. van Kessel, J. Phys. D 11, 1085 (1978)

II. THEORY OF LASER LIGHT ABSORPTION

§ 2.1 INTRODUCTION: THE WAVE EQUATION

If an electromagnetic wave is incident on an inhomogeneous plasma it is refracted and reaches a maximum electron density which depends on the angle of incidence, and which is given in case of normal incidence by $\omega = \omega_{pe}$, where ω is the frequency of the electromagnetic wave and

$$\omega_{pe} = \sqrt{\frac{e^2 N_e}{\varepsilon_o m_e}}$$ is the plasma frequency.

The electric field of the electromagnetic wave drives oscillations of the electrons in the plasma against the ion background; the oscillation energy is converted into thermal energy by electron-ion collisions. This process of absorption of radiation in the plasma is called collisional absorption or inverse bremsstrahlung. It is determined by the electron-ion collision frequency and by the penetration depth of the electromagnetic wave in the plasma.

An expression for the absorption rate of this process will be derived in § 2.2. Another absorption process occurs in isotropic inhomogeneous plasmas if the polarization of the electromagnetic wave is in the plane of incidence. This process, called linear mode conversion, will be touched upon in § 2.3; in case of linear mode conversion an electromagnetic wave is emitted at twice the frequency of the incident wave, which process will also be treated qualitatively in this paragraph. In addition the role of instabilities for absorption / reflection of the laser light will be discussed in § 2.4.

To describe the propagation of electromagnetic (EM) waves in a plasma we shall derive the wave equation. To this aim we use Maxwell's equations, which are in MKS units:

$$\begin{cases} \nabla \times \vec{E} = -\dfrac{\partial \vec{B}}{\partial t} & (2.1) \\ \nabla \times \vec{B} = \dfrac{\vec{j}}{\varepsilon_o c^2} + \dfrac{1}{c^2}\dfrac{\partial \vec{E}}{\partial t} & (2.2) \\ \nabla . \vec{B} = 0 & (2.3) \\ \nabla . \vec{E} = \dfrac{e}{\varepsilon_o}(N_i - N_e) & (2.4) \end{cases}$$

By elimination of $\vec{B}$ from eq. (2.1) and (2.2) we find:

$$\nabla \times \nabla \times \vec{E} + \frac{1}{c^2}\frac{\partial}{\partial t}\left\{\frac{\vec{j}}{\varepsilon_o} + \frac{\partial \vec{E}}{\partial t}\right\} = 0 \qquad (2.5)$$

where we have to find $\vec{j}$ as function of $\vec{E}$.

Therefore we need a description for the plasma; we shall use a so-called Lorentzian plasma, in which the ions are rigid: $M_i \gg m_e$ and the ion velocity is zero, $v_i = 0$. We can then write the <u>equation of motion</u> for the electrons

$$N_e m_e \left\{\frac{\partial \vec{v}_e}{\partial t} + (\vec{v}_e . \nabla)\vec{v}_e\right\} = -e N_e \left\{\vec{E} + \vec{v}_e \times \vec{B}\right\} + N_e m_e \nu_{ei}(\vec{v}_i - \vec{v}_e) \qquad (2.6)$$

and the current density is

$$\vec{j} = e N_e (\vec{v}_i - \vec{v}_e) = -e N_e \vec{v}_e \qquad (2.7)$$

Now we shall assume harmonic time dependence for all time functions, e.g.

$$\vec{E}(x, y, z, t) = \vec{E}(x, y, z)\, exp.(-i\omega t) \qquad (2.8)$$

Upon substitution in the equation of motion (2.6) and linearization we obtain $(-i\omega + \nu_{ei})\vec{v}_e = -\dfrac{e\vec{E}}{m_e}$

This is substituted in eq. (2.7)

$$\vec{j} = \frac{i}{\omega + i\nu_{ei}}\frac{e^2 N_e}{m_e}\vec{E}$$

Now we eliminate $\vec{j}$ from eq. (2.5) and find the wave equation

$$\Delta\vec{E} - \nabla(\nabla.\vec{E}) + k^2 n^2 \vec{E} = 0 \qquad (2.9)$$

where we have used $\nabla \times \nabla \times \vec{E} = -\Delta\vec{E} + \nabla(\nabla.\vec{E})$, and where $k = \omega/c$ is the vacuum wave vector.
The refractive index n is given by

$$n^2 = 1 - \frac{\omega_{pe}^2/\omega^2}{1 + i\nu_{ei}/\omega} \approx 1 - \frac{\omega_{pe}^2}{\omega^2} + i\frac{\omega_{pe}^2}{\omega^2}\frac{\nu_{ei}}{\omega} \qquad (2.10$$

and

$$\nu_{ei} = 3.63 \cdot 10^{-6} \; Z \ln\Lambda \; \frac{N_e(m^{-3})}{T_e(K)}$$

is the Spitzer electron-ion collision frequency. For laser-produced plasmas normally $\nu_{ei}/\omega < 0.1$.

We shall see that as long $Re(n^2) > 0$ we have propagating waves, whereas if $Re(n^2) \leq 0$ strong reflection occurs; if $\nu_{ei}/\omega << 1$, this reflection takes place at the point where the light frequency equals the plasma frequency, $\omega = \omega_{pe}$.

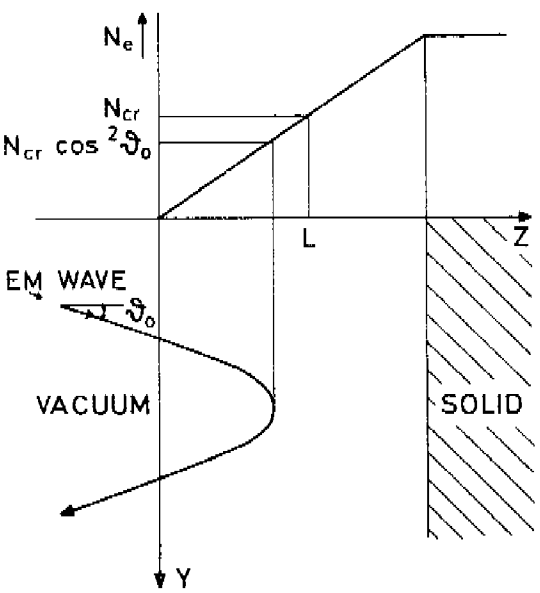

Fig. 2.1 An EM wave is incident at angle ϑ_0 into an inhomogeneous plasma. It is reflected at the density $N_{cr}\cos^2\vartheta_0$.

We write the wave equation (2.9) in cartesian components in order to solve it. We assume that the plasma is inhomogeneous in one direction: the z - axis. Then there is still one degree of freedom; we shall therefore choose the plane of incidence of the EM wave as yz - plane. The situation is drawn in Fig. 2.1.

We note, that the incident EM - wave is no function of the coordinate x; as the plasma is not dependent of x, the refracted EM-wave will also be independent of x; therefore all derivatives in eq. (2.9) with respect to x are zero. We have then for the components:

$$E_x : \quad \frac{\partial^2 E_x}{\partial y^2} + \frac{\partial^2 E_x}{\partial z^2} + k^2 n^2(z) E_x = 0 \qquad (2.11a)$$

$$E_y : \frac{\partial^2 E_y}{\partial y^2} + \frac{\partial E_y}{\partial z^2} - \frac{\partial}{\partial y}(\nabla . \vec{E}) + k^2 n^2(z) E_y = 0 \qquad (2.11b)$$

$$E_z : \frac{\partial^2 E_z}{\partial y^2} + \frac{\partial^2 E_z}{\partial z^2} - \frac{\partial}{\partial z}(\nabla . \vec{E}) + k^2 n^2(z) E_z = 0 \qquad (2.11c)$$

Now we distinguish between:

- <u>normal incidence</u>: the electric field has no z-component, at least if $n^2(z) \neq 0$ (this follows from eq. (2.11c) where $\partial/\partial y = 0$ for normal incidence).
- <u>oblique incidence</u>: as the inhomogeneity is only in z-direction, eq. (2.11a) is decoupled from eq. (2.11b) and (2.11c). Therefore during propagation in the plasma the EM wave keeps its polarization, and we distinguish:
  $\vec{E}$ is in x-direction: S-Polarization ("senkrecht" to the plane of incidence).
  $\vec{E}$ is in yz-direction: P-Polarization ("parallel" to the plane of incidence).

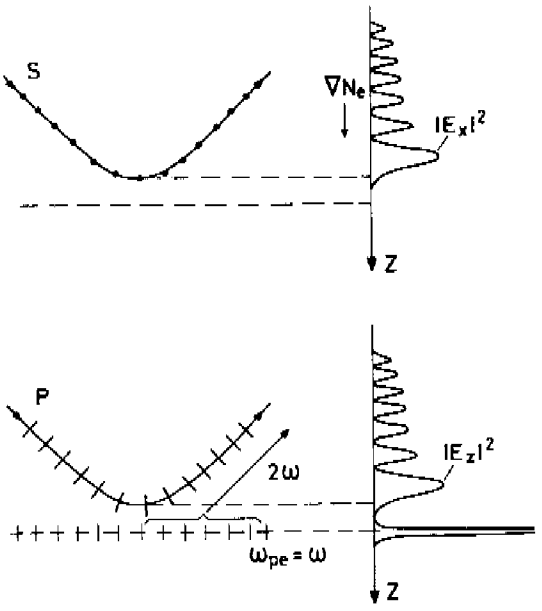

Fig. 2.2

a) Reflection of a S-polarized wave; the $\vec{E}$- vector is perpendicular to the paper. A standing wave pattern is formed with intensity $|E_x|^2$

b) Reflection of a P-polarized wave; a resonance occurs at $N_e = N_{cr}$; in addition a specular beam at frequency 2ω is emitted.

The reason for distinction between the two polarizations will become clear in the following. We shall confine ourselves at this moment to remark that a S-polarized wave will be reflected at the point where $n^2(z) = \sin^2 \vartheta_o$ and a standing wave with intensity $|E_x|^2$ will be formed: see Fig. 2.2a. A P-polarized wave, however, has an electric field-component parallel to the density gradient, and we shall see that in this case electrostatic waves are generated around the point $n^2(z) = 0$. The field structure is then of the form shown in Fig. 2.2b. The resulting process is called linear mode conversion. In addition a second harmonic wave (labeled 2ω in Fig. 2.2b) is generated at the critical density, where $\omega_{pe} = \omega$. This 2ω radiation is due to the resonance of the incident wave, and is in the direction of the reflected wave.

§ 2.2 S - POLARIZATION : INVERSE BREMSSTRAHLUNG

THE WKB - APPROXIMATION

In case of S-polarization the electric field has only a x-component, and is given by eq. (2.11a):

$$\frac{\partial^2 E_x}{\partial y^2} + \frac{\partial^2 E_x}{\partial z^2} + k^2 n^2(z) E_x = 0$$

Now we make an ansatz on the dependence of E_x on the coordinates y and z, based on the fact that the inhomogeneity is only in z direction

$$E_x(y,z) = F(z) \exp(\pm i k n(z) \sin\vartheta(z)\ y) \qquad (2.12)$$

$$= F \exp(\pm i k n \alpha y)$$

where $n = n(z)$

$\alpha = \sin\vartheta(z)$

By substitution in eq. (2.11a) we obtain:

$$\frac{d^2F}{dz^2} + k^2 n^2 (1-\alpha^2) F = \mp 2 i k y \frac{d(n\alpha)}{dz}\frac{dF}{dz} + \qquad (2.13)$$

$$\left[\mp i k y \frac{d^2(n\alpha)}{dz^2} + k^2 y^2 \left(\frac{d(n\alpha)}{dz}\right)^2\right] F$$

The RHS of eq. (2.13) has a factor y in all terms, the LHS is independent from y; as the equation must be valid for all y both sides must be equal zero and it follows:

$$\frac{d^2F}{dz^2} + k^2 n^2 (1 - \sin^2\vartheta) F = 0 \qquad (2.14)$$

$$\frac{d(n\alpha)}{dz} = 0 \quad \Longrightarrow \quad n \sin\vartheta = \text{constant} \qquad (2.15)$$

At the boundary of the plasma, at z = +0 we have $n(+0) = 1$ and $\vartheta = \vartheta_0$, therefore eq. (2.15) can be written $n \sin\vartheta = \sin\vartheta_0$, which is the Snellius law.

This gives in eq. (2.14)

$$\frac{d^2F}{dz^2} + k^2\left(n^2 - \sin^2\vartheta_0\right) F = 0 \qquad (2.14a)$$

For abbreviation we shall use $m = (n^2 - \sin^2\vartheta_0)^{1/2} = n\cos\vartheta$ as an "effective" refractive index.

We shall now discuss an approximative solution of eq. (2.14a), which is called the first approximation of geometrical optics or the WKB method. In a homogeneous medium m would be a constant. The solution of eq .(2.14a) would then be $F = c_1 e^{imz} + c_2 e^{-imz}$
The approximation of geometrical optics states that propagation in an inhomogeneous medium is approximately equal to propagation in a homogeneous medium with variable refractive index. Therefore we put as a solution

$$F(z) = F_0(z)\, e^{-ik\psi(z)} \qquad (2.15)$$

where $F(z)$ and $\psi(z)$ are slowly varying functions of z. If we put this in eq. (2.14a) we obtain:

$$F_0'' - 2ik\psi' F_0' - ik\psi'' F_0 + k^2\left[m^2 - (\psi')^2\right] F_0 = 0 \qquad (2.16)$$

with $F_0' = \frac{dF_0}{dz}$, $\psi' = \frac{d\psi}{dz}$ etc.

If the inhomogeneity has a characteristic scale length L which is much larger than a vacuum wavelength $\lambda/L \ll 1$ with $\lambda = 2\pi c/\omega = 2\pi/k$, we can split eq. (2.16) in orders 0, λ/L and λ^2/L^2 ; this gives

order 0: $$m^2 - (\psi')^2 = 0 \qquad (2.17a)$$

order λ/L $$2\psi' F_0' + \psi'' F_0 = 0 \qquad (2.17b)$$

The solution of eq. (2.17a) is $\psi = \pm \int m\,dz$

Then F_o is solved from eq. (2.17b)

$$F_o = \frac{c}{\sqrt{\psi'}} = \frac{c}{\sqrt{m}}$$

The general solution for F is then:

$$F = \frac{c_1}{\sqrt{m}} \exp\left(+ik\int_{z_o}^{z} m\,dz\right) - \frac{c_2}{\sqrt{m}} \exp\left(-ik\int_{z_o}^{z} m\,dz\right) \qquad (2.18)$$

At this point we remark:

- By developing eq. (2.16) in λ/L we have stopped at order λ^2/L^2 ; this means that $F_o'' \approx 0$, in other words: $m(z) = n(z)\cos\vartheta(z)$ should only change "slowly".
- We notice that if $m(z)$ goes to zero, the solution (2.18) breaks down.

We can look more quantitatively to the validity of solution (2.18) from eq. (2.14a) by noticing that (2.18) would be an <u>exact</u> solution if the effective refractive index in eq. (2.14a) would be of the form

$$\tilde{m}^2 = m^2 + \frac{1}{4k^2}\left[2\frac{m''}{m} - 3\left(\frac{m'}{m}\right)^2\right] = m^2 + m_1^2 \qquad (2.19)$$

in other words: as long as $|m_1^2/m^2| \ll 1$ solution (2.18) is a good approximation for eq. (2.14a).

At the other hand, if we are interested in the reflection of waves we cannot use the WKB approximation: this gives a linear superposition of two counter-propagating <u>independent</u> waves. Reflection will occur in the region where the condition $|m_1^2/m^2| \ll 1$ does not hold. Therefore we go back to equation (2.14a).

THE STOKES EQUATION

We shall solve now eq. (2.14a) for a linear density profile. Therefore we return to Fig. 2.1, where a wave is obliquely incident under an angle ϑ_o into an inhomogeneous plasma; the refractive index is given by eq. (2.10). We normalize the electron density to the critical density, where $\omega_{pe}=\omega$; from this we obtain $N_{cr} = \omega^2 \varepsilon_o m_e / e^2$. Then we write

$$\frac{\omega_{pe}^2}{\omega^2} = \frac{N_e}{N_{cr}}$$

and define the normalized collision frequency A as $A = (\nu_{ei})_{N_{cr}} / \omega$, where A is not a function of N_e anymore.
With this we write (compare (2.10))

$$n^2 = 1 - \frac{N_e}{N_{cr}} + iA \frac{N_e^2}{N_{cr}^2} \qquad (2.20)$$

A linear density profile is given by

$$\begin{cases} N_e = 0 \;, & z < 0 \\ N_e = \frac{z}{L} N_{cr} \;, & z \gg 0 \end{cases} \qquad (2.21)$$

where $L = \left\{ \frac{1}{N_e} \frac{dN_e}{dx} \right\}^{-1}_{N_{cr}}$ is the density scale length at N_{cr}

If we put this in eq. (2.20) and substitute n^2 in eq. (2.14a) we find for a linear density profile and $z \gg 0$

$$\frac{d^2F}{dz^2} + k^2 \left(\cos^2\vartheta_o - \frac{z}{L} + iA \frac{z^2}{L^2} \right) F = 0 \qquad (2.22)$$

Equation (2.22) can be transformed into the Stokes equation /1,2/ by a coordinate transformation, which can be applied around the place where $N_e = N_{cr} \cos^2\vartheta_o$ (the so-called cut-off density), if we linearize $n^2 = \cos^2\vartheta_o - \frac{z}{L} + iA\frac{z^2}{L^2}$
By linearization

$$n^2_{lin} = \cos^2\vartheta_o - \frac{z}{L} + iA\cos^2\vartheta_o \left(\frac{2z}{L} - \cos^2\vartheta_o \right) = a - b\frac{z}{L} \qquad (2.23)$$

a and b are constants, given by

$$a = \cos^2\vartheta_o \left(1 - iA\cos^2\vartheta_o\right)$$

$$b = 1 - i2A\cos^2\vartheta_o$$

Equation (2.22) can now be written:

$$\frac{d^2F}{dz^2} + \frac{k^2 b}{L}\left(\frac{aL}{b} - z\right)F = 0 \qquad (2.24)$$

Introducing a new space coordinate ζ by

$$\zeta = \left(\frac{k^2 b}{L}\right)^{1/3}\left(\frac{aL}{b} - z\right) \qquad (2.25)$$

the Stokes equation can be written:

$$\boxed{\frac{d^2F}{d\zeta^2} + \zeta F = 0} \qquad (2.26)$$

The solution of this equation is given by two sets of Airy functions $Ai(\zeta)$ and $Bi(\zeta)$ /2, 3/, where $Ai(\zeta)$ is evanescent in the overdense region ($\zeta < 0$), and $Bi(\zeta)$ diverges there; the solution of our problem is therefore given by $Ai(\zeta)$, which has an asymptotic expansion for large ζ (underdense region), given by

$$Ai_2 = \frac{1}{2}\pi^{1/2}\zeta^{-1/4}\left[e^{i\eta} + ie^{-i\eta}\right], \quad \eta = \frac{2}{3}\zeta^{3/2} \qquad (2.27)$$

As is computed in /2/, the relative error in $|(Ai - Ai_2)/Ai|$ becomes smaller than 4 % if $|\zeta| \geq 1.0$. Further we see in eq. (2.27) that Ai_2 is a WKB-like formula (2.18). This is clear, since for large ζ the approximation of geometrical optics must be valid.

By this requirement that expressions (2.18) and (2.27) should be identical for small z (large ζ), we can compute the reflection of a wave incident from a remote point z_o, where the WKB approximation is valid. If we assume that the incident wave is unity, and the reflected wave has the amplitude S, then from the condition that the electric field is continious we have:

$$\frac{1}{\sqrt{m}}\exp\left(+ik\int_{z_o}^{z} m\,dz\right) + \frac{S}{\sqrt{m}}\exp\left(-ik\int_{z_o}^{z} m\,dz\right) \qquad (2.28)$$

$$= C\,\frac{1}{2}\pi^{-1/2}\zeta^{-1/4}\left[i\exp(-i\eta) + \exp(i\eta)\right]$$

In this equation the incident wave on the LHS $(+ik\int\dots)$ must be equal to the incident wave on the RHS $(-i\eta)$ and equally the reflected waves. By eliminating the constant c we obtain the reflectance for the intensity:

$$R = ss^* = \exp 4\left(-\eta_i + k\int_z^{z_0} m_i\, dz\right) \qquad (2.29)$$

with $\eta_i = Im(\eta)$, $m_i = Im(m)$

We can now compute the reflectance for the linear density profile: from the definition of η , eq. (2.25) and (2.27), we find:

$$\eta = \frac{2}{3} kL\left(1 - i2A\cos^2\vartheta_0\right)^{1/2}\left(\cos^2\vartheta_0 - \frac{z}{L} + \frac{iA\cos^4\vartheta_0}{1 - i2A\cos^2\vartheta_0}\right)^{3/2}$$

if now: 1) $|A\cos^2\vartheta_0| \ll 1$ (normally $A < 0.1$)

2) $\left|\cos^2\vartheta_0 - \frac{z}{L}\right| \gg A\cos^4\vartheta_0$, which is valid if we stay away from the cut-off density where $z = L\cos^2\vartheta_0$

we can linearize η , and obtain for η_i :

$$\eta_i = kLA\cos^5\vartheta_0\left[\frac{\zeta_R^{1/2}}{(kL)^{1/3}} - \frac{2}{3}\,\frac{\zeta_R^{3/2}}{kL}\right] \qquad (2.30)$$

with $\zeta_R = (kL)^{2/3}\left(1 - \frac{z}{L\cos^2\vartheta_0}\right)$

The second part of expression (2.29) is the integral $k\int_z^{z_0} m_i\, dz$
Here the boundaries are the following:
z_0 should be somewhere in the underdense plasma, we make $z_0 = +0$ (to avoid reflection at the vacuum-plasma boundary by the discontinuity in $\frac{dm}{dz}$ for $z = 0$.
z is so to choose that it fulfills two conditions:
1) the WKB approximation should be still valid,
2) the deviation of the linearized refractive index from the real one is still small.

For computation of the integral we approximate m_i if $m^2 = \alpha + i\beta$ by $m_i \approx \frac{1}{2}\frac{\beta}{\sqrt{\alpha}}$ if $\left|\frac{\beta^2}{\alpha^2}\right| \ll 1$; this is valid in our case; then $m_i = \frac{A z^2/L^2}{2\sqrt{\cos^2\vartheta_0 - \frac{z}{L}}}$

and

$$k\int_z^{+0} m_i\,dz = \frac{kLA\cos^5\vartheta_0}{2}\int_{x=\frac{z}{L\cos^2\vartheta_0}}^{+0}\frac{x^2}{(1-x)^{1/2}}\,dx = \tag{2.31}$$

$$kLA\cos^5\vartheta_0\left[-\frac{8}{15} + \frac{\zeta_R^{1/2}}{(kL)^{1/3}} - \frac{2}{3}\frac{\zeta_R^{3/2}}{kL} + \frac{1}{5}\frac{\zeta_R^{5/2}}{(kL)^{5/3}}\right]$$

Combining expressions (2.30) and (2.31) and substituting them in eq. (2.29) we obtain:

$$R = \exp\left[-\frac{32}{15}\,kLA\cos^5\vartheta_0\left(1 - \frac{3}{32}\,\frac{\zeta_R^{5/2}}{(kL)^{5/3}}\right)\right]$$

The term with $\zeta_R^{5/2}$ is, even for steep density profiles ($kL \approx 6$), negligible with respect to 1. In fact we even suppose that this contribution in order $\zeta_R^{5/2}$ from the integral is not outweighed by an identical term in η_i , because we have linearized m^2. The reflectance for a linear density profile is therefore:

$$\boxed{R_{lin} = \exp\left(-\frac{32}{15}\,kLA\cos^5\vartheta_0\right)} \tag{2.32}$$

Remark: we see that the connection ζ_R between the WKB approximation (integration until z) and the Airy solution does not appear in formula (2.32). One can, however, ask what the limits are for ζ_R . For the validity of the WKB approximation we have condition (2.19); this gives the minimum value for ζ_R , which is 1.0 if $|m_1^2/m^2| < 0.3$ At the other hand ζ_R should not be too large, because then the error in linearizing $m^2(z)$ will become large; for $\zeta_R = 1.0$ we find that the relative error in m^2 is 0.1. It is therefore possible to connect the two solutions.

In the same way as described above one can compute the reflectance for an exponential density profile (see Fig. 2.3),

where

$$N_e(z) = N_{cr} \exp[(z - z_{cr})/L] \tag{2.33}$$

This profile is important as a result of a plane isothermal rarefying plasma (chapter V). The reflectance is:

$$R_{exp} = \exp\left(-\frac{8}{3} kLA \cos^3 \vartheta_o\right) \tag{2.34}$$

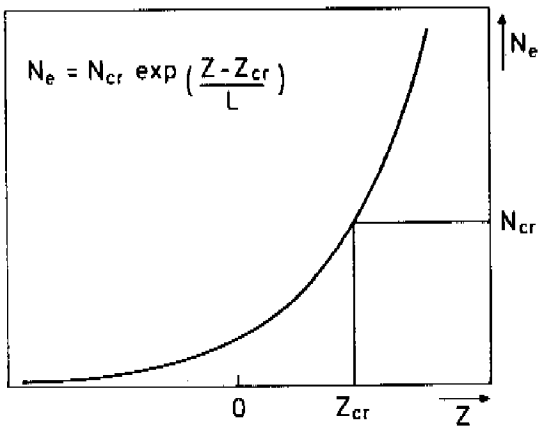

Fig. 2.3 Exponential electron density profile.

§ 2.3 P - POLARIZATION

LINEAR MODE CONVERSION

In the case of P-polarization the electric field of the incident EM wave has a component parallel to the density gradient $E_z \parallel \nabla N_e$. This field acts as a driver field and generates electrostatic oscillations at the critical density; the theory of this phenomenon, which is called linear mode conversion, or - less precise - resonance absorption is described in /1/. To give a qualitative picture of the mechanism we shall describe here an electrostatic $(\vec{B} = 0)$ condensator model /4/.

We start with the equation of continuity for the electrons, which we linearize; here n is the variation in the equilibrium density N_o, and v the oscillation velocity of the electrons ($v_{ions} = 0$). The equation is

$$\frac{\partial n}{\partial t} + \nabla . (N_o \vec{v}) = 0 \qquad (2.35)$$

The linearized equation of motion (2.6) gets, with $\vec{B} = 0$ and with $\vec{E}_D$ is the spatially uniform driver field:

$$\frac{\partial \vec{v}}{\partial t} + \nu_{ei} \vec{v} = - \frac{e}{m} (\vec{E} + \vec{E}_D) \qquad (2.36)$$

$\vec{E}$ follows from the Poisson equation (2.4): $\nabla . \vec{E} = - e n / \varepsilon_o$
We can solve these 3 equations for $\vec{E}$, remembering that $\omega_{pe}^2 = e^2 N_o / m_e \varepsilon_o$. The result is:

$$\nabla . \left\{ \frac{\partial^2 \vec{E}}{\partial t^2} + \nu_{ei} \frac{\partial \vec{E}}{\partial t} + \omega_{pe}^2 \vec{E} \right\} = - \nabla . \left\{ \omega_{pe}^2 \vec{E}_D \right\} \qquad (2.37)$$

We assume further harmonic time dependence for $\vec{E}_D$ (driver) and $\vec{E}$ (electrostatic) as $\sim \exp(-i\omega t)$; the density varies only in z-direction $N_e(z)$; the solution of eq. (2.37) is:

$$\vec{E} = \frac{\omega_{pe}^2 E_D}{\omega^2 - \omega_{pe}^2 + i \nu_{ei} \omega} \vec{e}_z \qquad (2.38)$$

note the resonance if $\omega_{pe} = \omega$. The absorbed flux of energy is now computed

$$I_{abs} = \int \frac{1}{2} \varepsilon_o |\vec{E}|^2 \nu_{ei} \, dz \qquad (2.39)$$

If we have a linear density gradient, $N_e / N_{cr} = \omega_{pe}^2 / \omega^2 = z/L$ then by substitution of $\vec{E}$ from eq. (2.38) in eq. (2.39) and integration we find:

$$I_{abs} = \frac{\pi \varepsilon_o}{2} |E_D|^2 \omega L \qquad (2.40)$$

We see that the absorbed flux is independent of the collision frequency: if ν_{ei} gets smaller the amplitude $|\vec{E}|$ in (2.38) increases, but the width of the resonance in (2.39) decreases, and the two effects cancel. Furthermore we note that the uniform driver field $\vec{E}_D$ must be in the z-direction, because otherwise the RHS in eq. (2.37) is equal zero: $\nabla \cdot (\omega_{pe}^2 (z) \vec{E}_D) = 0$. Therefore the resonance is only present if the driver is P-polarized.

For near normal incidence the component of $\vec{E}_D$ in z-direction is small, and therefore the absorption is small. For large angles of incidence ϑ_o the z-component of $\vec{E}_D$ is large, but the turning point given by $z = L \cos^2 \vartheta_o \ll L$, and only a small fraction of $\vec{E}_D$ can tunnel in to generate the resonance. Therefore there exists an optimum angle ϑ_m for resonance absorption, given by $(kL)^{2/3} \sin^2 \vartheta_m = 0.5$ The absorption curve, taken from /5/ is shown in Fig. 2.4.

The rigorous treatment of linear mode conversion differs from the electrostatic model that there the magnetic field is taken into account; the B - field provides the feed back determining the driver field E_D (in the electrostatic treatment the driver was an external field).

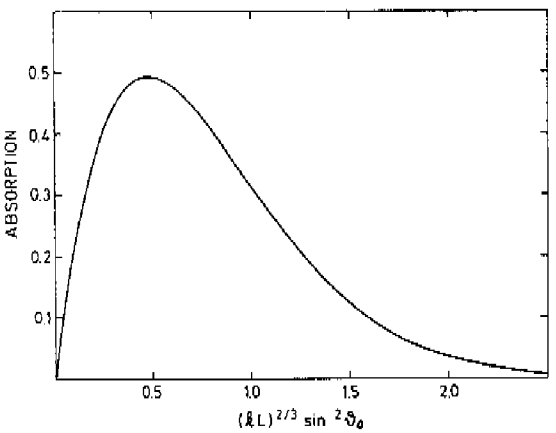

Fig. 2.4 Resonance absorption curve as computed by Kull in /5/.

In the context of linear mode conversion we want to stress one more point: the generation of suprathermal electrons by resonance absorption. As can be seen in eq. (2.38) the electric field can have a very high amplitude at resonance, and can thus accelerate electrons to high kinetic energies /6/. This may have a detrimental effect on the compression of DT pellets, as will be discussed in chapter V.

SECOND HARMONIC GENERATION

In the case of resonance absorption a second harmonic (SH) wave is generated at the critical density; it results from the nonlinearities in the motion of the electrons in the resonance field. The mechanism of second harmonic emission is described by Erokhin /7/.

The properties of second harmonic radiation follow from a simple argument. We assume harmonic time dependence of the form:

$$N_i = N_0 \quad \text{constant in time}$$

$$N_e = N_0 + n_1 \exp(-i\omega t) + n_2 \exp(-i2\omega t), \quad |n_2| \ll |n_1| \ll N_0$$

$$\vec{v}_i = 0 \quad \text{ions are rigid} \qquad (2.41)$$

$$\vec{v}_e = \vec{v}_0 + \vec{v}_1 \exp(-i\omega t) + \vec{v}_2 \exp(-i2\omega t), \qquad \vec{v}_0 = 0$$

(no zero-order current)

To be complete we should add the complex conjugates of all time functions (in order to obtain real time functions) but one can show that they do not modify the resulting SH source term (at least as long $|n_{i+1}| \ll |n_i|$). The current density is given by eq. (2.7)

$$\vec{j} = eN_e(\vec{v}_i - \vec{v}_e) = \tag{2.42}$$

$$-eN_0\vec{v}_1 \exp(-i\omega t) - e(n_1\vec{v}_1 + N_0\vec{v}_2)\exp(-i2\omega t)$$

$\vec{j}_2 = -e(n_1\vec{v}_1 + N_0\vec{v}_2)\exp(-i2\omega t)$ is the nonlinear source term

$\vec{v}_1$ and $\vec{v}_2$ are obtained from the equation of motion (2.6), where we have put $\nu_{ei} = 0$.

$$\frac{\partial \vec{v}_e}{\partial t} + (\vec{v}_e \cdot \nabla)\vec{v}_e = -\frac{e}{m_e}\vec{E} - \frac{e}{m_e}\vec{v}_e \times \vec{B}$$

With $\begin{cases} \vec{E} = \vec{E}_1 \exp(-i\omega t) + \vec{E}_2 \exp(-i2\omega t) \\ \vec{B} = \vec{B}_1 \exp(-i\omega t) \end{cases}$

we can solve for $\vec{v}_1$, and $\vec{v}_2$ by separating terms in ω and 2ω
The result is:

$$\vec{v}_1 = -\frac{ie}{m_e\omega}\vec{E}_1 \tag{2.43}$$
$$\vec{v}_2 = \frac{ie^2}{2m_e\omega^3}\left[(\vec{E}_1 \cdot \nabla)\vec{E}_1 + i\omega\vec{E}_1 \times \vec{B}_1\right] - \frac{ie}{2m_e\omega}\vec{E}_2$$

With Maxwell's equation (2.1) we finally find for $\vec{v}_2$:

$$\vec{v}_2 = \frac{ie^2}{2m_e^2\omega^3}\,\frac{\nabla(\vec{E}_1 \cdot \vec{E}_1)}{2} - \frac{ie}{2m_e\omega}\vec{E}_2 \tag{2.44}$$

Next n_1 follows from the equation of continuity (2.35), which is linearized

$$\frac{\partial n_1}{\partial t} + \nabla \cdot (N_0\vec{v}_1) = 0 \tag{2.45}$$

$\vec{v}_1$ is given by eq. (2.43) and $\vec{E}_1$ comes from $\nabla \cdot \vec{E}_1 = -\frac{e}{\varepsilon_0} n_1$
We find:

$$n_1 = \frac{e}{m_e\omega^2}\,\frac{(\vec{E}_1 \cdot \nabla N_0)}{1 - \omega_{pe}^2/\omega^2} \quad ; \qquad \omega_{pe}^2 = \frac{e^2 N_0}{\varepsilon_0 m_e} \tag{2.46}$$

Therefore $\vec{j}_2$ is given by:

$$\vec{j}_2 = -\frac{i e^2}{m_e^2 \omega^3}\left[\frac{\vec{E}_1(\vec{E}_1 \cdot \nabla N_0)}{1-\omega_{pe}^2/\omega^2} - \frac{N_0}{4}\nabla(\vec{E}_1 \cdot \vec{E}_1)\right] - \frac{i e^2 N_0 \vec{E}_2}{2 m_e \omega} \qquad (2.47)$$

The first two terms are sources for $\vec{j}_2$, the last term is the self-consistent electric field. We readily identify some important properties of the source term:

- in a spatially homogeneous plasma ($\nabla N_0 = 0$) the only remaining term is the second; since this term $\nabla(\vec{E}_1 \cdot \vec{E}_1)$ is longitudinal it does not excite transverse SH waves.
- the most important term in $\vec{j}_2$ is the first one; we recognize:

a) the resonant character if $\omega \to \omega_{pe}$;

b) there is only a contribution if $(\vec{E}_1 \cdot \nabla N_0) \neq 0$; therefore the incident wave must be P-polarized;

c) $\vec{j}_2$ is determined by the product $n_1 \vec{v}_1$: this is essentiellly larger than the contributions by $(\vec{v}_1 \cdot \nabla)\vec{v}_1$ and $\vec{v}_1 \times \vec{B}_1$. The SH is therefore generated by the oscillating electrons which act as radiating dipoles.

d) the first term in $\vec{j}_2$ scales with the incident intensity I_0 ($\sim E_1^2$), the emitted power at 2ω scales then with I_0^2

e) As the SH emission scales with the square of the incident intensity, it should also scale with the square of the resonance absorption function from Fig. 2.4 (see the treatment of SH generation in /7/).

§ 2.4 ABSORPTION / REFLECTION BY INSTABILITIES

Nonlinear wave-wave interactions can influence greatly the absorption of laser radiation in an inhomogeneous plasma. Nonlinear coupling of light to a medium is well known in nonlinear optics: the coupling is here caused by the nonlinear susceptibility of the medium. As can be seen in eq. (2.6), in laser-produced plasmas the plasma itself

causes the nonlinear coupling by the $(\vec{v}.\nabla)\vec{v}$ and $\vec{v}\times\vec{B}$ terms; because of the strong electric fields from the intense laser beam this coupling can be very efficient.

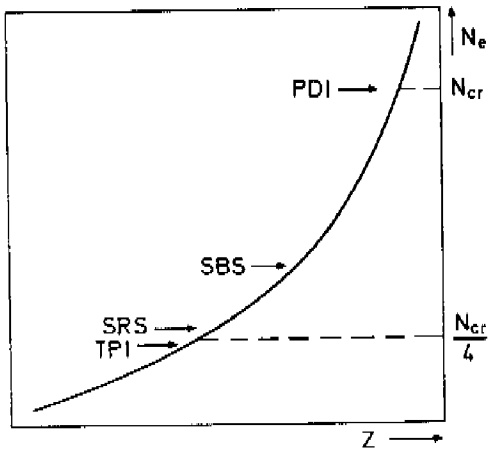

Fig. 2.5 Parametric instabilities are excited between $N_{cr}/4$ and N_{cr}, depending on the $(\omega, \vec{k})$ conservation laws. For the symbols see the text.

The most important interaction processes are (Fig. 2.5):

Stimulated Brillouin Scattering	SBS	$t \rightarrow t' + i$
Stimulated Raman Scattering	SRS	$t \rightarrow t' + e$
Parametric Decay Instability	PDI	$t \rightarrow e + i$
Two Plasmon Instability	TPI	$t \rightarrow e + e$

In this notation t (t') is the incident (reflected) EM wave, i is an ion wave, and e is an electron plasma wave. The conversion process should fulfill the energy and momentum conservation requirements:

$$\begin{cases} \omega = \omega_1 + \omega_2 \\ \vec{k} = \vec{k}_1 + \vec{k}_2 \end{cases}$$

In addition the Manley-Rowe relations prescribe which part of the driver-wave (ω) is transferred into the waves ω_1 and ω_2:

$$-\Delta\left(\frac{P_\omega}{\omega}\right) = \Delta\left(\frac{P_{\omega_1}}{\omega_1}\right) = \Delta\left(\frac{P_{\omega_2}}{\omega_2}\right)$$

The TPI and SRS are generated at density $N_e = N_{cr}/4$ where $\omega_{pe} = \omega/2$ these instabilities, as well as the PDI (generated at $N_e = N_{cr}/4$) can provide rather efficient light absorption. The picture for SBS is different: this instability can be excited in the underdense plasma, and from the

Manley-Rowe relations one can conclude that only a very small part of the incident energy is absorbed in the plasma ($\approx \omega_{ia}/\omega$ where ω_{ia} is the frequency of the ion acoustic wave). The rest of the energy is contained in the reflected EM wave; it's frequency differs only slightly from that of the incident EM wave, and upon backreflection into the laser chain it can be amplified (if the bandwidth of the amplifying medium is broad enough). Therefore it is believed that SBS may cause the principle loss mechanism in laser plasma coupling, and can even be dangerous for the laser system. SBS needs for amplification an extended underdense plasma; most experiments described in this thesis were performed with short pulses (30 ps), and steep density gradients. In addition the applied intensities on target ($\leqslant 10^{14}$ W/cm^2) make excitation of the instabilities improbable; at least during the experiments none of these instabilities was identified (in case of 30 ps pulses). Therefore we restrict ourselves in the following to the linear absorption mechanisms.

References of chapter II:

1. V.L. Ginzburg, The Propagation of Electromagnetic Waves in Plasmas (Pergamon, Oxford, 1970)

2. P. Mulser and C. van Kessel, J. Phys. D. 11, 1085 (1978)

3. M. Abramowitz and J.A. Stegun, Handbook of Mathematical Functions (Dover, New York, 1972)

4. W.L. Kruer, 20th Scottish Universities Summer School on Laser-Plasma Interactions, St. Andrews 1979

5. H. Kull, Max-Planck-Gesellschaft zur Förderung der Wissenschaften e.V. Report No. PLF 16/1979

6. J.P. Freidberg, R.W. Mitchell, R.L. Morse, and L.I. Rudinski, Phys. Rev. Lett. 28, 795 (1972)

7. N.S. Erokhin, V.E. Zakharov, and S.S. Moiseev, Zh. Eksp. Teor. Fiz. 56, 179 (1969) [Sov. Phys. JETP 29, 101 (1969)]

III. EXPERIMENTAL APPARATUS

§ 3.1 THE Nd/YAG LASER

The experiments, described in chapter IV, were performed with a Quantel Nd/YAG laser. It consists of an oscillator, a pulse selector system and 4 amplifiers. See Fig. 3.1.

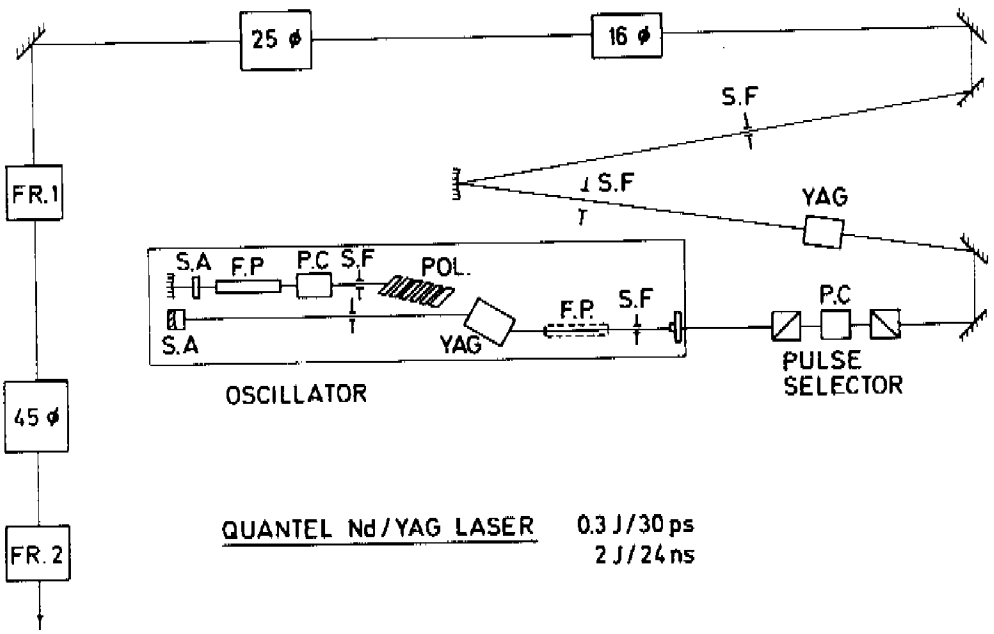

Fig. 3.1 Laser system for laser plasma interaction experiments.

The oscillator can be used in 2 branches: using it as a passively mode-locked oscillator (lower branch in Fig. 3.1) it generates pulse trains of about 10 pulses at intervals of 6 ns; the pulse length can be chosen with a revolving output mirror having 4 silica plates with different thicknesses, corresponding to pulse durations of 30, 50, 100 and 200 ps.

The active medium is a YAG crystal doped with Nd^{3+} ions. Passive mode-locking is achieved by a dye cell with a saturable absorber (labelled S.A.); 2 diaphragms are build in as spatial filters (S.F.) providing a single transverse TEM_{00} mode output. The oscillator can also be used for generating single longitudinal mode TEM_{00q} pulses of 24 ns FWHM duration. For this purpose a stack of plate polarizers can be put into the chain (upper branch). A Pockels cell (P.C.) forms together with the polarizer an active Q-switch; the longitudinal mode selection is made by 2 Fabry-Perot etalons (F.P.), the 5 mm thick output mirror, and a saturable absorber. A pulse selector, consisting of 2 Glan prisms and a spark gap triggered Pockels cell is used to select one pulse out of the pulse train from the ps-chain. The extinction ratio of this combination was measured 2×10^5. This provides sufficient target isolation against prepulses. The selected pulse is amplified in a Nd/YAG preamplifier, and (after 2 spatial filters) in 3 Nd glass amplifiers of 16, 25, and 45 mm diameter.

The chain is protected against backreflected light from the target by 2 Faraday rotators with total extinction ratio of 3×10^4. For target experiments with frequency doubled light there is no danger of amplification of the backreflected (0.53 µm) light in the amplifiers; therefore the Faraday rotators are not needed in this case. The polarization of the incident beam is linear and is better than 95 %. The energy of the laser system at $\lambda = 1.06$ µm on target is 0.3 J in 30 ps pulse duration, or 2 J in 24 ns. The repetition rate of the oscillator and preamplifier is one pulse every 3 seconds, for the total chain it is one shot every 2 minutes (firing at full power).

§ 3.2 FOCUSING OPTICS

To obtain the desired irradiance on target the laser light had to be focused. The focusing optics had to meet the following specifications:

to have a well collimated focused beam a large f/number lens should be used.
- the focus diameter should be small enough to reach the required intensities (10^{11} - 10^{14} W/cm^2), on the other hand it should be large enough that one could speak of a one-dimensional (plane) geometry (plasma expansion during the laser pulse should be small compared to the focal spot size).
- the lens should have the same properties for all applied wavelengths (1.06 μm, 0.53 μm, 0.26 μm).

The requirements were fulfilled with an achromatic f/8, 400 mm focal length for 1.06 μm and 0.53 μm, and a similar lens made out of quartz for 0.26 μm. The focal spot size was measured by focusing through pinholes. We used the following technique. First the focus position was determined by a Hartmann-plate (see /1/): a mask with holes was placed in front of the focusing lens; by firing the laser chain a picture of the mask was produced on photographic paper near the focus. In this way the axial focus position could be determined with $\pm$ 50 μm accuracy. This should be compared with the Rayleigh range, which was 1 cm. Then we fired the laser with full power, and focussed the attenuated beam on a 5 μm thick Al-foil. With a first shot a hole was created, and at a second shot the energy transmitted through this hole was measured with an energy detector. By firing several times through a hole we found that the percentage transmitted energy remained constant, i.e. the hole size did not increase (e.g. by plasma production on the edge of the hole). After the shots the hole sizes were measured under a microscope. The results for λ = 0.53 μm are presented in Fig. 3.2. It appeared that 50 % of the energy was concentrated in a spot of 40 μm diameter, resulting in maximum intensity on target of 3 x 10^{14} W/cm^2. Very similar spot sizes were obtained at the other wavelengths. It should be stressed that these measurements - as all experiments - were made with the "warm" laser chain: after 5 shots

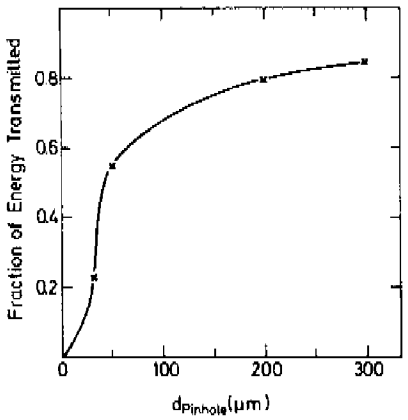

Fig. 3.2 Fraction of the incident laser energy transmitted through pinholes. The wavelength of the laser is 0.53 μm, it is focussed by a f/8, 400 mm lens.

at constant interval of 2 minutes the focal position was stabilized, which was clear from the transmission measurements.

The position of the target was controlled by means of a 60 x projection of the back of the targets; this method provided an accuracy of target positioning of ± 15 μm.

§ 3.3 FREQUENCY CONVERSION

If an electromagnetic wave is incident on a solid, the material will be polarized: in every molecule an electric dipole moment is induced, which for weak fields is proportional to the incident electric field; this follows from the fact that for weak fields the electrons can be considered as harmonic oscillators. The resulting polarization is then linear proportional to the electric field. For strong fields, however, the oscillations of the electrons may not be pure harmonic anymore, and the polarization has a nonlinear component proportional to some higher power of the electric field. Thus if the electromagnetic wave has the frequency ω the polarization will have a component varying with 2ω . This nonlinear effect can be used for upconversion of the frequency of laser beams of high intensity,

in which the electric field is strong (some MV/cm).

Frequency doubling and quadrupling of 1.06 µm laser radiation can be achieved efficiently with the crystals KH_2PO_4 and KD_2PO_4 (abbreviated KDP and KD*P). In these crystals the nonlinear susceptibility is nonzero, and upon irradiation with a strong electromagnetic wave a nonlinear polarization is induced. An expression for the second harmonic conversion is given in Yariv's book /2/: the nonlinear polarization enters as a source term in the wave-equation . By solving it one obtains an expression for the conversion efficiency

$$\eta = \frac{P_{2\omega}}{P_\omega} = 2\left(\frac{\mu_o}{\varepsilon_o}\right)^{3/2} \omega^2 \frac{d_{36} \sin\vartheta_m}{n^3} L^2 I_\omega \left\{\frac{\sin\frac{\Delta k L}{2}}{\Delta k L/2}\right\}^2 \qquad (3.1)$$

here d_{36} is the tensor element of the nonlinear susceptibility,

ϑ_m is the angle between the optic axis and the propagation direction

$P_{\omega,2\omega}$ is the power of the beam at frequency ω, 2ω

n is the refractive index

Δk = $k_{2\omega} - k_\omega$ is the mismatch between the propagating second harmonic and fundamental beams

L is the crystal length.

I_ω = P_ω / Area is the intensity of the fundamental beam

This expression is only valid as long as the conversion efficiency is small. We shall verify the dependence of η on the parameters in eq. (3.2) for the crystals used in the experiments.

For conversion from λ = 1.06 µm to 0.53 µm we used two different crystals: for short pulses (30 - 200 ps) a 1.7 cm length KDP type II crystal was used; its conversion efficiency was 40 %. For long pulses (24 ns) a 4.5 cm length deuterated KD*P II crystal was applied; because of the long pulses, and smaller incidence power, its conversion was somewhat lower, 30 %.

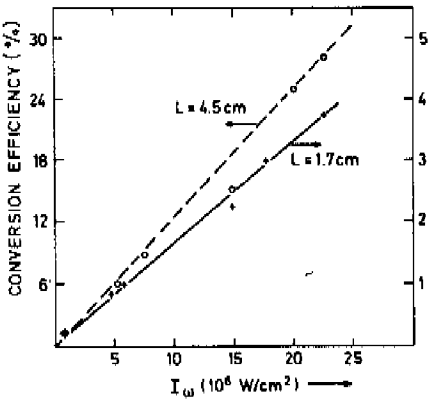

Fig. 3.3a Conversion efficiency $P_{2\omega}/P_\omega$ as function of incidence intensity I_ω for a 4.5 cm and a 1.7 cm length crystal. Incident beam has λ = 1.06 μm and 24 ns pulse duration.

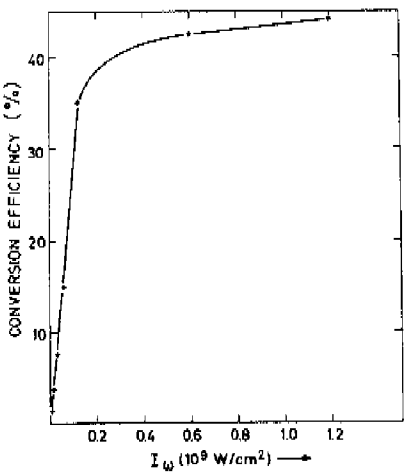

Fig. 3.3b Conversion efficiency from 0.53 μm to 0.26 μm as function of incidence intensity I_ω and for 30 ps pulses. Crystal length is 1 cm.

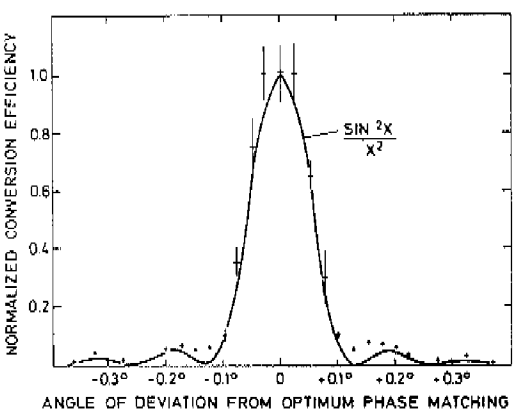

Fig. 3.3c Decrease of conversion efficiency (normalized to the maximum) by misalignment of the frequency doubling crystal.

The dependence of η on crystal length and incidence intensity is seen from Fig. 3.3a. Here the conversion efficiency from 1.06 μm to 0.53 μm is plotted against incidence intensity for the 4.5 cm crystal (left scale, dashed curve) and the 1.7 cm crystal (right scale, solid curve). We notice

- η scales linearly with I_ω, in agreement with eq. (3.2)
- the conversion efficiency for the longer crystal is 7 times as high as for the short crystal; this is in agreement with the quadratic scaling of L: $(4.5 / 1.7)^2 \approx 7$.

For further conversion from λ = 0.53 μm to 0.26 μm a KDP type I crystal was used. Characteristic for this conversion step is that the crystals are relatively short (our crystal had a length of 1 cm) and that high intensity I_ω is needed to obtain a good efficiency: Fig. 3.3b. A conversion efficiency of 45 % was obtained for this step.

The effect of phase-mismatch ($\Delta k \neq 0$) is plotted in Fig. 3.3c. It shows the decrease in conversion efficiency from 0.53 μm to 0.26 μm by minor misalignment of the angle between the fundamental beam and the phasematch direction. The experimental points are compared with the $(\frac{\sin x}{x})^2$ curve from eq. (3.2).

§ 3.4 DIAGNOSTICS FOR LASER-PLASMA INTERACTIONS

The object of the experiments was to obtain a clear picture of the absorption mechanisms in laser-produced plasmas. To determine the absorption we have measured the reflectance R, which is the fraction of the light reflected from the plasma; from this one calculates the absorbed fraction (A) by A = 1 - R. The diagnostics in our experiments can be divided in two groups:

- fast diagnostics of the temporal pulse shape of the laser beam
- slow diagnostics of the energy incident and reflected from the laser-produced plasma.

The first group consists mainly of fast vacuum photodiodes, which record the shape of the laser pulse: double pulses due to imperfect mode-locking and occasional transmission of more than one pulse by the pulse selecting system are detected. Their time resolution is 1 ns. Prepulses $< 10^{-2}$ of the main pulse cannot be resolved with a single vacuum photodiode; if their intensity on target exceeds some 10^{10} W/cm^2 (depending on the target material) they can damage the target. For detection of these prepulses a combination of a fast Si p-i-n photodiode with a 20 dB Avantek preamplifier has been applied, which is drawn in Fig. 3.4. The total bandwidth of the circuit is 1 GHz. Prepulses $\gtrsim 10^5$ W (corresponding to at maximum 5 x 10^9 W/cm^2 on target) are detected. Pulses $> 10^8$ W, which saturate the amplifier, are detected with the vacuum photodiodes. For measurements with very high time resolution a streak camera is used, which has a time resolution of 10 ps.

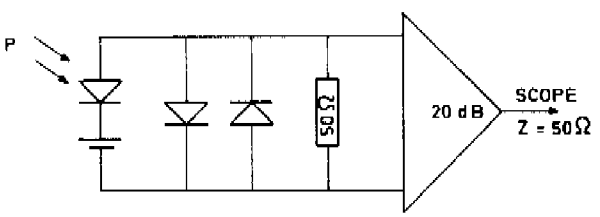

Fig. 3.4 Prepulse detector; the photodiode operates in reverse way. Upon irradiation with a light impulse P it transmits an electric impulse in the HF amplifier.

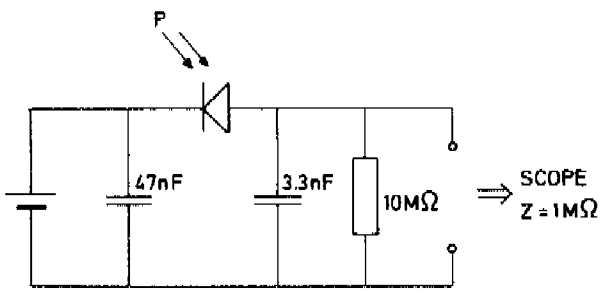

Fig. 3.5 Photodiode operating as an energy detector.

The energies at various positions in the laser chain, and the energy incident and reflected from the target are recorded with Si p-i-n diodes with integrators: Fig. 3.5. The inverse current through the diode is proportional to the light incident on the diode; the output signal is a step voltage with a rise time $\tau_1 \approx 30$ µs and a long decay time τ_2 of 3 ms. The energydiodes are calibrated absolutely against Gentec energymeters, and have proven to be very accurate detectors. The diodes are protected with diffusing ground-glass, so that their calibration is not too sensitive on the direction of the incident light.

The energy diodes are suitable diagnostics for recording collimated (specularly) reflected light; for measurements of the total amount of light reflected from the target the light should be collected in a solid angle of 4π sr. For this purpose we have used an Ulbricht integrating sphere /3,4/. See Fig. 3.6. It consists of a hollow sphere of 15 cm diameter. Its inner surface is coated with Eastman White

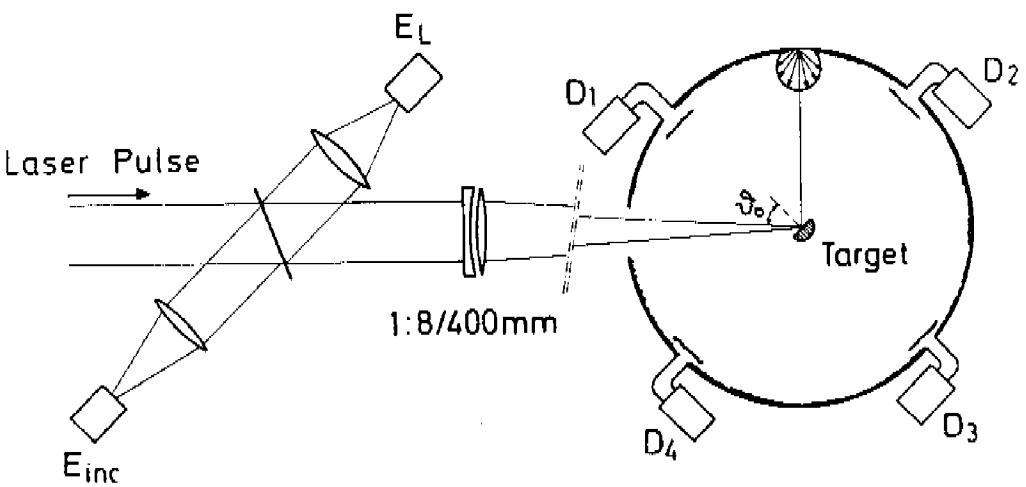

Fig. 3.6 Ulbricht spherical photometer for total reflectance measurements.

Reflectance paint, which reflects the light isotropically; it's reflectance for wavelengths between 0.26 µm and 1.06 µm is high ($\geq$ 0.96). Less than 2 % of the sphere surface is taken in by apertures for focusing and imaging the target. As detectors 4 Si-diodes (from Fig. 3.5) are placed symmetrically in the lower part of the sphere; they have screens to prevent them for seeing directly reflected light from the laser irradiated target. The sphere is calibrated by firing into the empty sphere; the signals of the energy diodes are then normalized against the incident energy and averaged. The response of the sphere is found to be intensity independent from 0 - 300 mJ (corresponding to intensities on the wall of the sphere less then 1.5 GW/cm^2) as can be seen from Fig. 3.7a. Deviations from the line-

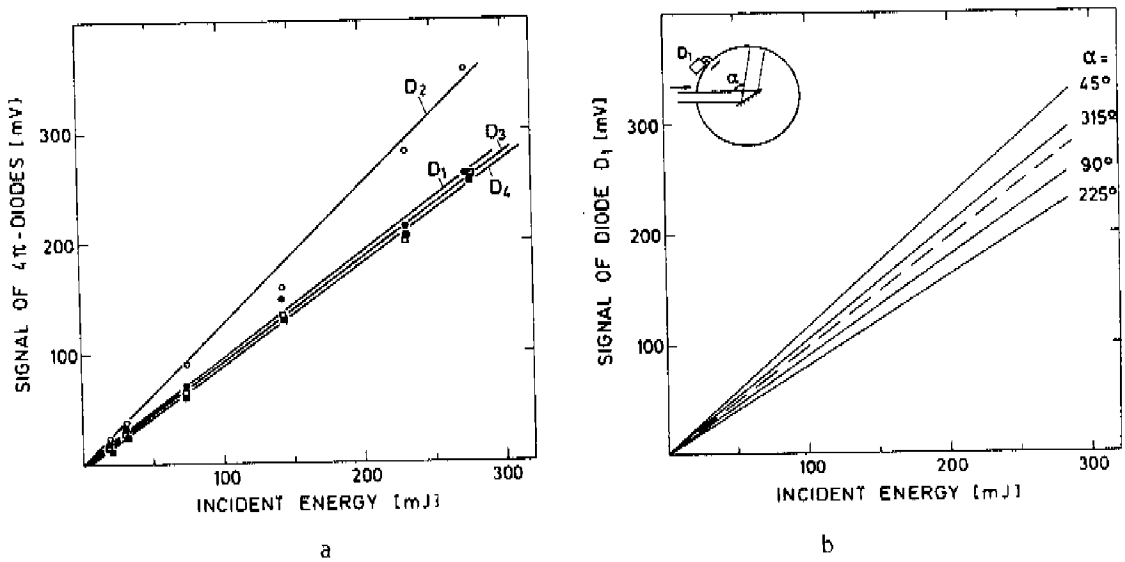

Fig. 3.7 a) Signals of the diodes D_1, D_2, D_3 and D_4 as function of incident energy; λ = 0.53 µm.
b) Signal of diode D_1 as function of incident energy; λ = 0.53 µm. The dashed curve is obtained without mirror (from a). The solid curves are for different illumination angles to the sphere wall.

arity are smaller than 6 %. At intensities > 2 GW/cm^2 plasma is created on the wall, resulting in a less than linear response. The angular dependence of the diodes has been tested by placing a 99.8 % reflecting dielectric mirror in the centre of the sphere, and firing on it with a parallel beam. By attenuating the incident energy and by rotating the mirror w.r.t. the laser axis the response of each diode has been measured; in Fig. 3.7b the signal of diode D_1 is plotted in dependence of incident energy, and for different angles α . For comparison we have drawn a dashed line, which is the signal of D_1 from Fig. 3.7a, i.e. its response for calibration of the empty sphere. We see from Fig. 3.7b that the deviation from the dashed line for different angles is at maximum 18 %: the signal of D_1 is maximum if the light reflects in its neighbourhood (α = 45°), and minimum if the reflection lies at the opposite side of the sphere (α = 225°); it is clear that this deviation is greatly reduced if we average over the 4 diodes. Concluding we find that the angular and intensity dependence of the Ulbricht sphere + diodes is smaller than $\pm$ 5 %.

References of chapter III:

1. K. Eidmann, G. Brederlow, P. Brodmann, R. Sigel, R. Volk, S. Witkowski, and K.J. Witte, Max-Planck-Gesellschaft zur Förderung der Wissenschaften e.V. Report No. PLF 4/1978.

2. A. Yariv, Quantum Electronics, 2nd ed., (Wiley, New York 1975), chapter 16.

3. R. Ulbricht, Elektrotechn. Z. 21, 595 (1900); see also L. Bergmann and C. Schaeffer, Lehrbuch der Experimentalphysik, Band III, Optik (de Gruyter, Berlin 1974) p.629.

4. R.P. Godwin, P. Sachsenmaier, and R. Sigel, Phys. Rev. Lett. 39, 1198 (1977).

IV. EXPERIMENTAL RESULTS

§ 4.1 Comparative Reflectance Measurements on Laser-Produced Plasmas at 1.06 μm and 0.53 μm.
Phys. Rev. Lett. 42, 1625 (1979)

§ 4.2 Reflectance Measurements on Laser-Produced Plasmas at 0.26 μm.
Opt. Commun. 33, 62 (1980)

§ 4.3 Second Harmonic Generation Accompanying Linear Mode Conversion in a Laser-Produced Plasma
to be published in Opt. Commun.

§ 4.4 Resonance Absorption of a Wavelength-shifted Probe Beam in a Laser-Produced Plasma
submitted to Z. Naturforsch.

Comparative Reflectance Measurements on Laser-Produced Plasmas at 1.06 and 0.53 μm

A. G. M. Maaswinkel, K. Eidmann, and R. Sigel
Projektgruppe für Laserforschung der Max-Planck-Gesellschaft zur Förderung der Wissenschaften e.V., D-8046 Garching bei München, Germany

(Received 28 March 1979)

The total and specular reflectances of 1.06- and 0.53-μm laser pulses were measured on planar copper targets. The measurements were made with 30-ps pulses and an intensity on target of 10^{14} W/cm^2. The direction of polarization and angle of incidence (0°–70°) were varied. Only a weak dependence of reflectance on wavelength is found; at both wavelengths reflectance is governed by the characteristic angle and polarization dependence of resonance absorption.

Absorption and reflection of intense laser radiation on solid targets is a basic problem in laser-fusion studies. A crucial parameter in this respect is the wavelength of the laser. Up to now, most laser plasma experiments have been made with the CO_2 (10.6 μm), Nd (1.06 μm) and iodine lasers (1.315 μm). No systematic studies, however, have been undertaken in the shorter-wavelength region, although considerable effort is being made to develop visible and near-uv lasers. In this Letter we present measurements of the total and specular reflectances at 1.06 and 0.53 μm and pulse duration of 30 ps. Since recent measurements[1-4] suggest that resonance absorption is an important absorption mechanism, we have studied in detail the dependence of reflectance on the angle of incidence and polarization of the incident laser light. Much attention has been paid to ensuring identical experimental conditions at both wavelengths to allow comparison of the results.

The laser is a Nd:YAlG (neodymium-doped yttrium aluminum garnet) system delivering 0.7 J in 30 ps. A high-contrast Pockelscell-Glan prism combination (extinction ratio 2×10^5) guarantees a clean pulse (prepulses are <6 μJ). For measurements at 1.06-μm isolation against back-reflected light and rotation of the polarization is achieved by two Faraday rotators; the resulting energy on target is 300 mJ. For 0.53-μm generation we use a potassium dihydrogen phosphate type-II crystal of 51 mm in diameter and 17 mm in length. Its conversion efficienty is 40%, giving 200–300 mJ on target. The polarization here is rotated with a $\lambda/2$ plate. At both wavelengths the polarization is better than 95%. The laser light is focused on target by an achromatic 1:8/400-mm lens. The focal spot was measured by focusing through pinholes.[5] It contains 50% of the energy in a spot 40 μm in diameter, resulting in an averaged intensity on target of 3×10^{14} W/cm^2. Our 30-ps pulse, the total angle of the lens of 7°, and a Rayleigh range of 1 cm will enable us to approach a plane geometry in our experiments. Note that with $t=30$ ps and an estimated temperature of $T_e=400$ eV the plasma expands over a distance $L_H=t(Zk_BT_e/m_i)^{1/2}\approx4$ μm during the laser pulse, i.e., a distance much smaller than the focal-spot diameter. The experiments were done on Cu targets, made from highly polished hemicylindrical steel rods with 2-μm-thick Cu coatings.

It is known that one obtains in general, upon reflection from a plane target, three components of reflected laser light with characteristic angular distributions[6]: (i) a well-collimated, specular beam (R_{spec}) with a divergence similar to that of the incident beam, (ii) diffusely scattered laser light (R_{diff}) with a very broad angular distribution, and (iii) so-called collimated backscatter through the focusing lens due to Brillouin backscattering. In our case the last component was found to be negligible ($<10^{-2}$), at least for angles of incidence larger than 3.5° (the half-angle of the lens) where it can be discriminated against the specular beam. This is probably due to our short pulse duration and correspondingly small plasma size where no substantial amplification of the backscattered component can occur. With an Ulbricht spherical photometer as described previously in[4] we measured first the total reflection coefficient $R_{tot}^{s,p}=R_{spec}^{s,p}+R_{diff}$; s,p stands for the polarization of the beam. Here we integrate over a solid angle of 4π steradians; the light reflected through the lens and the incident energy were measured separately with photodiodes. We improved the accuracy of the sphere by using four Si p-i-n diodes as detectors; their average signal is accurate to <5%. The response of the sphere is independent of the incident energy from 0 to 300 mJ.[5] Its calibration was checked before and after each series of measurements.

In order to know the contribution of the specular and diffuse components, we have to measure one of them separately. We measured $R_{spec}^{s,p}$

with the Ulbricht sphere removed. Tests with burnpaper showed immediately that a well-defined specular beam is produced upon reflection. Quantitatively its energy was measured with a Gentec detector. The solid angle covered by this detector. The solid angle covered by this detector was varied using a diaphragm of variable diameter in the range 2×10^{-2} to 1.2×10^{-1} sr (14°–38° one angle). This did not change the detector signal. Hence the energy of the specular beam is indeed contained in a divergence angle similar to that of the incident beam; on the other hand, we can conclude that the diffusely scattered light has a much broader angular distribution. This measurement of the specular beam energy together with the Ulbricht-sphere measurements then allows us to calculate $R_{\mathrm{diff}}^{s,p}=R_{\mathrm{tot}}^{s,p}-R_{\mathrm{spec}}^{s,p}$.

The result of the reflectance measurements are plotted in Figs. 1 and 2. The data points are mean values for at least ten shots up to twenty shots. The measurements were made with the focus on target, with intensity $(1-3)\times10^{14}$ W/cm^2. At 1.06 μm (Fig. 1) a maximum absorption of 0.43 occurs for p-polarized light at an angle of incidence of $\vartheta=20°$. There is a good agreement between this curve and that obtained by Godwin *et al.* in Ref. 4. We notice that 30% of the energy is still absorbed at $\vartheta=0°$.

At $\lambda=0.53$ μm, absorption is always somewhat higher. At $\vartheta=0°$ it is about 0.40, similar to that in Ref. 7; it reaches a maximum of 0.62 for p polarization also at 20° incidence. At both wavelengths a pronounced difference between s- and p-polarized radiation is evident. It is also clear from Figs. 1 and 2 that in general a strong component of diffusely scattered light is present. It dominates reflection losses at normal incidence (0°), but decreases with increasing angle of incidence. Its intensity depends only weakly on the polarization of the incident beam. A comparison of Figs. 1 and 2 shows that the diffuse component at a fixed angle (22°) is reduced for $\lambda=0.53$ μm as compared to 1.06 μm (at $\lambda=1.06$ μm and $\vartheta=0°$ we have $R_{\mathrm{diff}}^{s,p}=0.55$). Additional measurements have shown that R_{diff} decreases with decreasing intensity.

The observed angle and polarization dependence is believed to be due to resonance absorption.[2,4] A complication arises from the presence of diffuse scattering which is not taken into account in the usual theory of resonance absorption. In this situation a fractional absorption due to resonance absorption may be defined as $f_{\mathrm{res}}=(R_{\mathrm{spec}}^{s}-R_{\mathrm{spec}}^{p})/R_{\mathrm{spec}}^{s}$. With this definition only the fractional energy absorbed out of the *specular* beam due to the polarization effect is attributed to resonance absorption. In Fig. 3 the data of Fig. 2 are plotted in this way and compared with a theoretical curve as calculated by Ginzburg.[8,9] There is fair agreement up to the maximum $f_{\mathrm{res}}\approx0.5$ for $\vartheta=20°$, but for larger angles the experimental absorption is larger than calculated. The same observation

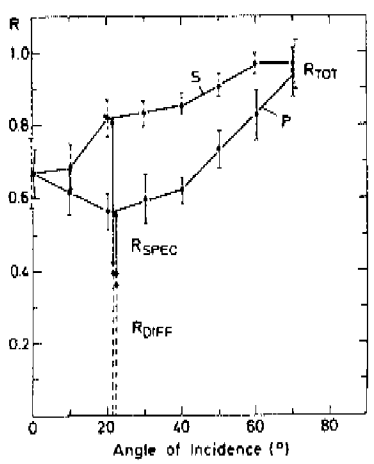

FIG. 1. Reflectance R_{tot} into 4π steradians as a function of the incidence angle for s- and p-polarized light and $\lambda=1.06$ μm. Specular reflectance R_{spec} measured at $\vartheta=22°$. Intensity on target is $(1-3)\times10^{14}$ W/cm^2.

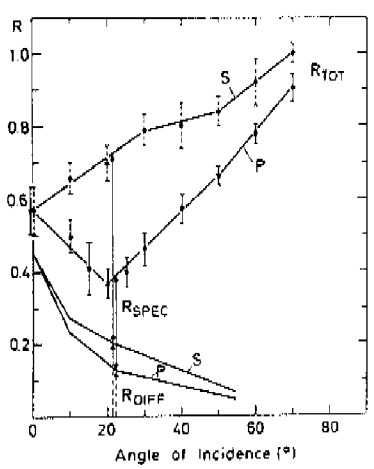

FIG. 2. Reflectance R_{tot}, and R_{spec} at $\vartheta=0°$, 10°, 22°, and 55° for $\lambda=0.53$ μm. Intensity is $(1-3)\times10^{14}$ W/cm^2.

was made more indirectly by Balmer *et al.*[3] From Fig. 1 one obtains $f_{rcs} = 0.52$ at 22° in agreement with the result at $\lambda = 0.53$ μm. We have also made another set of measurements for $\lambda = 1.06$ and 0.53 μm at 10^{11} W/cm^2. The characteristic polarization dependence remains unchanged, though reflectance decreases, possibly as a result of collisional absorption (for example maximum total absorption is 0.65 at $\lambda = 1.06$ μm and 0.82 at $\lambda = 0.53$ μm). If all these results are plotted as in Fig. 3 they coincide within the error bars with the experimental curve shown there. Thus we have the important result that the resonant part of absorption is *independent of wavelength and intensity* as it is expected to be. Maximum absorption occurs for both wavelengths at $\vartheta_m = 20°$. One may obtain[8] from this angle the scale length L of the density gradient by $(2\pi L/\lambda_0)^{1/3} \sin\vartheta_m = 0.7$. One finds $L = \lambda_0$ *both* wavelengths, in agreement with previous observations at $\lambda = 1.06$ μm.[1-4]

Resonance absorption in a smooth plasma layer cannot explain the observed absorption at normal incidence. If total absorption at 1.06 μm would be due to collisional absorption, it should increase more strongly than observed for 0.53 μm. Estimates with[10,11] $T_e = 400$ eV and $L = \lambda$ show that an absorption of 10% at 1.06 μm and 20% at 0.53 μm may be attributed to collisional absorption; the major source of absorption most likely has other causes. The observation of strong diffuse scattering at normal incidence suggests that absorption is connected with the underlying "roughness" of the reflecting plasma layer. As has been discussed in Thomson, Kruer, and Langdom[12] resonance absorption may account for nearly all of the absorption in the presence of roughness.

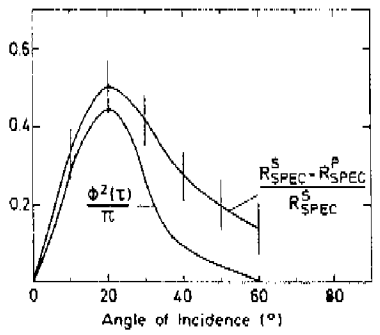

FIG. 3. Comparison at $\lambda = 0.53$ μm between theoretical resonance absorption $\varphi^2(\tau)/\pi$ and the experimental curve obtained from Fig. 2.

Also it seems important to remember that coupling to surface plasmons leads to enhanced light absorption on rough metal surfaces.[13] This effect which is bascially similar to resonance absorption is of interest at least as a limiting effect for a plasma with a very steep density gradient. In contrast to a metal surface, roughness in a laser-produced plasma is, however, generated by the interaction itself and therefore the situation is extremely complicated. At the present time, the cause and importance of diffuse scattering in the context of resonance absorption is difficult to assess; it still surprises us that the predicted behavior of resonance absorption is so readily distilled out of a more complex situation.

In conclusion, a comparative investigation of laser-light absorption has revealed a very similar behavior at $\lambda = 1.06$ and 0.53 μm. Absorption is dominated by resonance absorption; we have verified its three main characteristics: (i) angle and polarization dependence, (ii) independence of intensity, and (iii) independence of wavelength. Resonance absorption is thus found to be an important mechanism at infrared *and* visible wavelengths.

The authors acknowledge the skillful technical assistance of P. Sachsenmaier and E. Wanka. This work was supported in part by the Bundesministerium für Forschung und Technologie and EURATOM. One of us (A.G.M.M.) acknowledges receipt of a EURATOM grant.

[1]J. S. Pearlman and M. K. Matzen, Phys. Rev. Lett. 39, 140 (1977).

[2]K. R. Manes, V. C. Rupert, J. M. Auerbach, P. Lee, and J. E. Swain, Phys. Rev. Lett. 39, 281 (1977).

[3]J. E. Balmer and T. P. Donaldson, Phys. Rev. Lett. 39, 1084 (1977).

[4]R. P. Godwin, P. Sachsenmaier, and R. Sigel, Phys. Rev. Lett. 39, 1198 (1977).

[5]A. G. M. Maaswinkel, K. Eidmann, and R. Sigel, Max-Planck-Gesellschaft zur Förderung der Wissenschaften eV, Report No. PLF-10/1978 (unpublished).

[6]See, for example, the discussion of experiments by B. H. Ripin, Naval Research Laboratory Memorandum Report No. 3684, 1977 (unpublished).

[7]F. Amiranoff, R. Benattar, R. Fabbro, E. Fabre, C. Garban, C. Popovics, A. Poquerusse, R. Sigel, C. Stenz, J. Virmont, and M. Weinfield, in *Proceedings of the Seventh International Conference on Plasma Physics and Controlled Nuclear Fusion Research, Innsbruck, Austria, 1978* (International Atomic Energy Agency, Vienna, Austria, 1978), paper IAEA-CN-37-D-4.

[8]V. L. Ginzburg, *The Propagation of Electromagnetic Waves in Plasmas* (Pergamon, Oxford, 1970), p. 267.
[9]K. G. Estabrook, E. J. Valeo, and W. L. Kruer, Phys. Fluids 18, 1151 (1975).
[10]J. W. Shearer, Phys. Fluids 14, 183 (1971).
[11]T. W. Johnston and J. M. Dawson, Phys. Fluids 16, 722 (1973).
[12]J. J. Thomson, W. L. Kruer, A. Bruce Langdon, Claire Ellen Max, and W. C. Mead, Phys. Fluids 21, 707 (1978).
[13]Julian Crowell and R. H. Ritchie, J. Opt. Soc. Am. 60, 794 (1970).

REFLECTANCE MEASUREMENTS ON LASER-PRODUCED PLASMAS AT 0.26 μm

A.G.M. MAASWINKEL
Projektgruppe für Laserforschung der Max-Planck-Gesellschaft zur Förderung der Wissenschaften e.V., D-8046 Garching bei München, Federal Republic of Germany

Received 28 January 1980

Total and specular reflection from planar Al-targets was measured with a frequency-quadrupled (λ = 0.26 μm) Nd-YAG laser. The intensity on target was 4×10^{13} W/cm^2 with pulse duration 20 ps. Total absorption for near normal incidence was 80%, very little dependence on intensity and pulse duration was found. By varying the polarization and angle of incidence (0° - 80°) the characteristic behaviour of resonance absorption was observed.

Reflection losses from a laser-produced plasma are a matter of concern for laser fusion. Experiments performed so far at infrared wavelengths of 1.06 μm, 1.3 μm and 10.6 μm show high reflection losses with typical absorption of only 30 - 40%. It is expected that absorption increases at shorter wavelengths where a denser and cooler plasma will be produced. Recent experiments in the visible at λ = 0.53 μm have indeed shown an increase in absorption [1 - 4]. Here we present results obtained in the UV at λ = 0.26 μm. Such short wavelengths may be of practical interest since powerful UV lasers like the KrF-laser (λ = 0.25 μm) might become available in the future.

We have measured the total and specular reflectance from planar targets. The experimental set-up was basically the same as described in [3], to facilitate the comparison of results at the different wavelengths. The beam of the frequency-doubled Nd-YAG laser was further up converted to 0.26 μm with a potassium dihydrogen phosphate type I crystal of 45 mm diameter and 10 mm length. The upconversion efficiency was 45%. The 0.53 μm light was blocked with dielectric filters (transmission $T_{0.26\,\mu m} = 0.7$, $T_{0.53\,\mu m} = 10^{-4}$). The light was focused with a 40 cm Suprasil lens with effective aperture 1:40. The pulse duration at 1.06 μm was 30 ps and at 0.26 μm was estimated as 20 ps. The energy on target was 20 mJ; focal spot size measurements showed 70% transmission through a 50 μm pinhole. This resulted in an averaged intensity on target of 4×10^{13} W/cm^2.

The total reflectance was measured with the Ulbricht spherical photometer [3]; the inside of the sphere was covered with Eastman White Reflectance Paint which is a good diffusor for light between 0.2 - 2.5 μm. As detectors, four Si p-i-n diodes with quartz windows were used. During calibration the linearity and reproducibility of the averaged signal was measured and found to be better than ±5%.

For measurements of the specular reflectance the Ulbricht sphere was removed. We measured the light reflected specularly with a p-i-n diode with diffusor. It observed the light in a solid angle of 5×10^{-4} sr; this is only slightly larger than that of the incident beam. In addition the incident light and the light backreflected through the focusing lens was measured with an identical detector.

We were careful to choose a target with well characterized optical properties. As a standard target we used Al-mirrors with a 0.15 μm protective MgF-coating; at 0.26 μm its reflectance at low intensity of 10^7 W/cm^2 (no plasma) was measured to be 70% into specular direction. No diffuse scattering due to surface roughness was observed in tests with the Ulbricht sphere. We are therefore confident that the high absorption found upon irradiation of the target indeed comes from the plasma.

Fig. 1 shows the total reflectance R_{tot} of an Al/MgF-target as function of the angle of incidence, obtained as the sum of the light scattered into the Ulbricht sphere and back into the focusing lens. Only

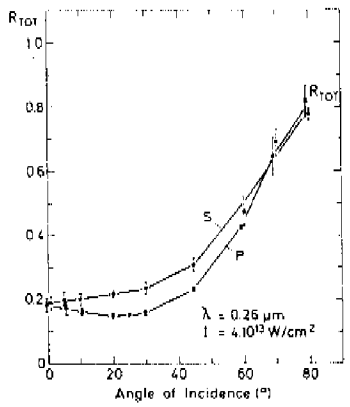

Fig. 1. Total reflectance R_{tot} into 4π sterad as function of the angle of incidence for s- and p-polarization at $\lambda = 0.26\ \mu m$.

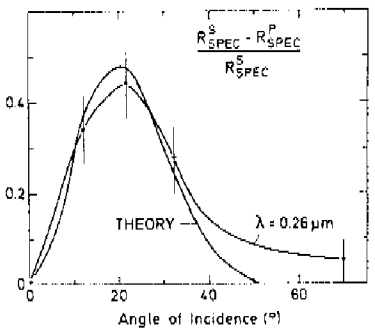

Fig. 2. Comparison between theoretical resonance absorption (from [5]) and the experimental curve obtained from the specular reflectance for s- and p-polarization.

a small fraction, $R_{tot} \approx 0.2$, is reflected for angles $\vartheta \leqslant 40°$, i.e. the plasma formed upon irradiation of the target is highly absorbing at the applied wavelength of $\lambda = 0.26\ \mu m$. There is also a difference in reflectance between s- and p-polarized light though less pronounced than in previous curves measured at $\lambda = 1.06\ \mu m$ and $0.53\ \mu m$. We found that the low reflectance shown in fig. 1 was not very sensitive to the experimental conditions. Reducing the intensity to 2×10^{11} W/cm^2 (by defocusing) gave a total reflectance of 0.15. With a longer laser pulse of 200 ps (nominal for $1.06\ \mu m$, estimated to 150 ps for $0.26\ \mu m$) at intensity 8×10^{12} W/cm^2 we found $R_{tot} = 0.13$. Finally no dependence of reflectance on target material was seen for Al/MgF, Cu and glass targets. There are no indications for enhanced backscatter due to Brillouin scattering through the lens for the short pulses applied here, as one would expect from corresponding observations at 1.06 and 0.53 μm [3]. Even in the case of occasional double pulsing the second pulse was more strongly absorbed than the first one.

Of particular interest is the angular variation of the reflectance for the specular beam, R^s_{spec} and R^p_{spec} for s- and p-polarization respectively. The specular reflectance is measured with the Ulbricht sphere removed. In order to reveal better the role of resonance absorption we have plotted in fig. 2 the ratio $(R^s_{spec} - R^p_{spec})/R^s_{spec}$. The theoretical curve was in this case taken from numerical calculations by Kull [5]. One sees a good agreement between the curves, as was observed previously at $1.06\ \mu m$ and $0.53\ \mu m$. The set of measurements at 2×10^{11} W/cm^2 was found also to be in accordance with the theoretical curve.

We interpret the results as follows: in comparison with $\lambda = 1.06\ \mu m$ and $0.53\ \mu m$ absorption at $0.26\ \mu m$ is considerably higher. This is not unexpected, since the higher plasma density and presumably lower temperature would suggest an increase of collisional absorption in the plasma. Quantitatively, however, it is still difficult to assess the fractional absorption due to this mechanism, since it depends on the density profile and temperature of the plasma which are not accurately known. In any case the weak dependence of absorption on the target material, pulse length and intensity suggests that these results may be also relevant for a larger parameter regime, not accessible in this experiment. It is inferred from fig. 1 that the contribution of resonance absorption is relatively weak at $0.26\ \mu m$ as compared to 1.06 and $0.53\ \mu m$. This is an interesting result in the context of laser fusion since a decrease of fast electron production may be expected under such conditions. On the other hand, as the special plot in fig. 2 shows, the contribution for resonance absorption can still be identified very well. As for the case of 1.06 μm and $0.53\ \mu m$, the measured and calculated curves are in good agreement; in particular a maximum of ~50% is absorbed out of the specular beam as expected. We note that the measured curve in fig. 2 peaks at $\vartheta \approx 20°$; the same angle was found at $1.06\ \mu m$ and $0.53\ \mu m$. Since the maximum of the resonance curve

is given by $(2\pi L/\lambda)^{1/3} \sin\vartheta \approx 0.7$, we find with $\vartheta \approx 20°$ at all three wavelengths $L \approx \lambda$, i.e. the density scale length L is about equal to one vacuum wavelength. Such steep gradients have been verified interferometrically at 1.06 μm [6,7] and 10.6 μm laser wavelength [8]. Finally we recall that the curve of fig. 2 was also obtained at 2×10^{11} W/cm^2. Hence the independence of resonance absorption of wavelength and intensity is confirmed once more by these measurements.

The author acknowledges numerous discussions with Dr. Sigel and the technical assistance of E. Wanka. He also acknowledges receipt of a EURATOM grant. This work was supported in part by the Bundesministerium für Forschung und Technologie and EURATOM.

References

[1] A.G.M. Maaswinkel, K. Eidmann and R. Sigel, Max-Planck-Gesellschaft zur Förderung der Wissenschaften e.V. Report No. PLF 10/1978 (unpublished).
[2] F. Amiranoff, R. Benattar, R. Fabbro, E. Fabre, C. Carban, C. Popovics, A. Poquerusse, R. Sigel, C. Stenz, J. Virmont and M. Weinfeld, in: Proc. 7th Int. Conf. on Plasma physics and controlled nuclear fusion research, Innsbruck, Austria 1978 (IAEA, Vienna, Austria, 1978) paper IAEA-CN-37-D-4.
[3] A.G.M. Maaswinkel, K. Eidmann and R. Sigel, Phys. Rev. Lett. 42 (1979) 1625.
[4] F. Amiranoff, R. Fabbro, E. Fabre, C. Carban, J. Virmont and M. Weinfeld, Phys. Rev. Lett. 43 (1979) 522.
[5] H. Kuli, Max-Planck-Gesellschaft zur Förderung der Wissenschaften e.V. Report No. PIF 16/1979 (unpublished).
[6] D.T. Attwood, D.W. Sweeney, J.M. Auerbach and P.H.Y. Lee, Phys. Rev. Lett. 40 (1978) 184.
[7] A. Raven and O. Willi, Phys. Rev. Lett. 43 (1978) 278.
[8] R. Fedosejevs, M.D.J. Burgess, G.D. Enright and M.C. Richardson, Phys. Rev. Lett. 43 (1979) 1664.

Second Harmonic Generation Accompanying Linear Mode Conversion in a Laser-produced Plasma.

A.G.M. Maaswinkel

Projektgruppe für Laserforschung der Max-Planck-Gesellschaft zur Förderung der Wissenschaften e.V.
D-8046 Garching, Fed. Rep. of Germany

Abstract

Second harmonic (SH) generation in a laser produced plasma (NdYAG laser with wavelength 1.06 μm, pulse duration 30 ps, intensity 10^{13} Wcm^{-2}) was investigated experimentally as a function of polarization and angle of incidence of the laser beam. The results are in agreement with theoretical predictions for SH generation in the presence of linear mode conversion in the plasma.

In the context of laser fusion there is a considerable interest in linear mode conversion /1/ also called resonance absorption as an intensity and wavelength independent absorption mechanism. Absorption of laser light due to this mechanism, in particular the characteristic polarization and angle dependence, has recently been investigated experimentally in considerable detail /2-5/.

It is theoretically predicted that linear mode conversion should be accompanied by second harmonic (SH) emission from the irradiated plasma /6-8/ which should bear as well the characteristic features of it. In fact, in an early paper Eidmann and Sigel /9/ have verified, at least qualitatively, the polarization and angle dependence of SH emission accompanying linear mode conversion. Nevertheless, it seems desirable, especially on the background of the progress made recently with investigations of linear mode conversion, to attempt a more quantitative verification of SH emission by this mechanism. In particular a quantitative measurement of SH conversion efficiency as a function of the angle of incidence could yield complementary information with respect to linear mode conversion. If the present understanding of the absorption experiments is correct, the angular variation of SH emission should follow the square of the Ginzburg absorption curve /1/ which has been found to describe absorption experiments /2-5/. Such a measurement is the purpose of this investigation. It is important to note that the measurements are made with an apparatus which has been used previously for absorption measurements/3/; thus a quantitative comparison of SH emission and absorption by linear mode conversion is possible.

Briefly the apparatus (already described in /3/) has the following characteristics: the plasma is produced by short (30 ps) pulses from a Nd YAG laser (λ = 1.06 µm). Occasional prepulses $>$ 6 µJ could be detected with a Si p-i-n diode and 10 dB preamplifier with a total bandwidth of 1 GHz. The polarization of the laser beam at the target could be

changed by means of a $\lambda/2$ - plate, and the degree of polarization (s or p) was checked to be better than 95 %. The incident 1.06 μm light and the (specularly) emitted SH light were recorded with Si p-i-n diodes with interference filters. The light was focussed with a 400 mm lens, with effective aperture 1 : 20. The targets were highly polished mirrors with 2 μm Cu coating.

The theoretical description applies to a planar geometry where SH emission should occur into the direction of specular reflection. In order to verify this we recorded the angular distribution of SH light with a 2π ellipsoidal mirror as described in /10/; the mirror surface was photographed with a Polaroid camera. A well defined SH beam with an angular width about equal to the incident (and reflected) fundamental beam was indeed observed for a focal spot of 250 μm diameter (and larger). When the focal spot was made smaller (by moving the focus onto the target surface) the distribution of SH light became more diffuse; the SH beam was more sensitive in this respect than the reflected fundamental beam. Rather diffuse SH emission was also observed in the case of occasional double pulses from the laser. The focal spot diameter was finally fixed at 250 μm, corresponding to an intensity of $2 \times 10^{13} Wcm^{-2}$. The photographs showed the striking polarization dependence of SH emission: bright spots were observed for p-polarization but disappeared for s-polarization.

The mirror in conjunction with a spectrograph served also to measure the spectrum of the emitted SH beam. Within the resolution of the spectrograph (3 Å) the SH frequency was exactly equal to twice the frequency of the fundamental beam and no broadening was detectable, indicating that other SH generation mechanisms, in particular scattering of plasmons generated by parametric instabilities (see the

review /11/), are not important in our case. For quantitative measurements the mirror was replaced by a Si-diode photodetector with appropriate filters; it observed the SH light in a solid angle of 6.10^{-3} Sr which is 3 x the incident solid angle. The SH detector was calibrated absolutely against a Gentec energymeter; for this purpose we upconverted the Nd-laser with a KDP-II crystal. In this manner we could determine the absolute SH conversion in the plasma.

The dependence of SH emission on polarization and angle of incidence is shown in Fig. 1. Each data point is an average over 10 shots. In addition we have measured the absolute SH conversion as a function of the incident laser energy for p-polarized light at an angle of incidence of 22° (Fig. 2). The focal spot was kept constant for this measurement; the energy was attenuated with filters.

According to theory /6-8/ SH emission should vary with the angle of incidence as the square of the Ginzburg absorption curve. The theoretical curve in Fig. 1 comes from taking the square of the particular curve which has been previously found to represent the best fit to the experimentally measured absorption curve (/3/ maximum at 22°). As is seen the angular variation of SH emission is indeed well described by it. Also, except for a spurious, weakly angle dependent background emission in the case of s polarization, SH emission occurs only for a p-polarized laser beam as expected. We note that we also confirmed these results with a 1 mm diam. focal spot corresponding to an intensity of $1o^{12}Wcm^{-2}$.

Fig. 2 shows that the SH energy scales approximately with the square of the laser energy as expected. The experimental maximum conversion was 3.10^{-6}. It is difficult to compare this with the theoretical value, as the latter depends strongly on the density scale length L and the effective

collision frequency ν_{eff} /6/, which is not known. However, with a value $L \approx \lambda$, obtained from the SH curve, and a reasonable value $\nu_{eff}/\omega \approx 0.02$ we find theoretical values for the conversion similar to the experimental numbers.

In summary we have found that linear mode conversion in a laser produced plasma is accompanied by SH emission with the characteristic dependence on polarization, angle of incidence and intensity theoretically predicted.

The author is indebted to Dr. Sigel for his helpful advices during this investigation, and to Mr. Wanka for assistance during the experiments.
He acknowledges receipt of a Euratom Grant.
This work was supported in part by the Bundesministerium für Forschung und Technologie and by Euratom.

References

/1/ V.L. Ginzburg, The Propagation of Electromagnetic Waves in Plasmas (Pergamon, Oxford 1970), p. 267

/2/ K.R. Manes, V.C. Rupert, J.M. Auerbach, P. Lee, and J.E. Swain, Phys. Rev. Lett. 39, 281 (1977)

/3/ A.G.M. Maaswinkel, K. Eidmann, and R. Sigel, Phys. Rev. Lett. 42, 1625 (1979)

/4/ A.G.M. Maaswinkel, Opt. Commun. 33, 62 (1980)

/5/ E. Fabre, J. Virmont, F. Amiranoff, R. Fabbro, C. Garban, and M. Weinfeld, 21st APS Meeting, Division of plasma Physics, Boston 1979

/6/ N.S.Erokhin, V.E. Zakharov, and S.S. Moiseev, Zh. Eksp. Teor. Fiz. 56, 179 (1969) [Sov. Phys. JETP 29, 101 (1969)]

/7/ N.S. Erokhin, S.S. Moiseev, and V.V. Mukhin, Nucl. Fusion 14, 333 (1974)

/8/ G. Auer, K. Sauer, and K. Baumgärtel, Phys. Rev. Lett. 42, 1744 (1979)

/9/ K. Eidmann, and R. Sigel, Phys. Rev. Lett. 34, 799 (1975)

/10/ R.P. Godwin, C.G.M. van Kessel, J.N. Olsen, P. Sachsenmaier, R. Sigel, and K. Eidmann, Z. Naturforsch. 32a, 1100 (1977)

/11/ N.G. Basov, V.Yu. Bychenkov, O.N. Krokhin, M.V. Osipov, A.A. Rupasov, V.P. Silin. G.V. Sklizkov, A.N. Starodub, V.T. Tikhonchuk, and A.S. Shikanov, Kvantovaya Elektron. (Moscow) 6, 1829 (1979) [Sov. J. Quantum Electron. 9, 1081 (1979)]

Figure Captions

Fig. 1 Energy of SH light ($E_{2\omega}$) for s-and p-polarization in dependence of the angle of incidence. The intensity on target was $2.10^{13} W/cm^2$. The theoretical curve (see text) is normalized to the experimental result.

Fig. 2 Energy of SH light ($E_{2\omega}$) as a function of the incident laser energy (E_{ω}); p-polarization, angle of incidence 22°.

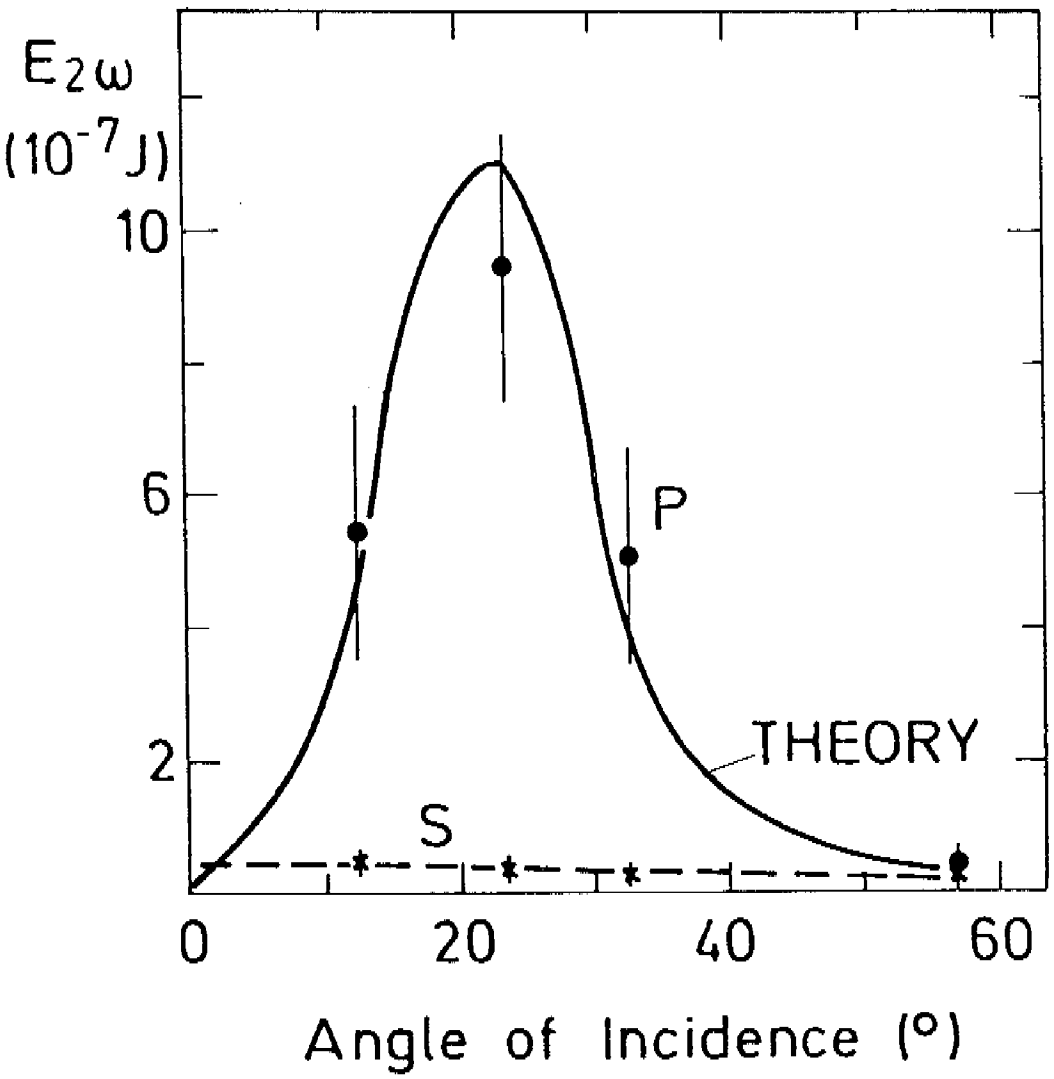

Fig. 1

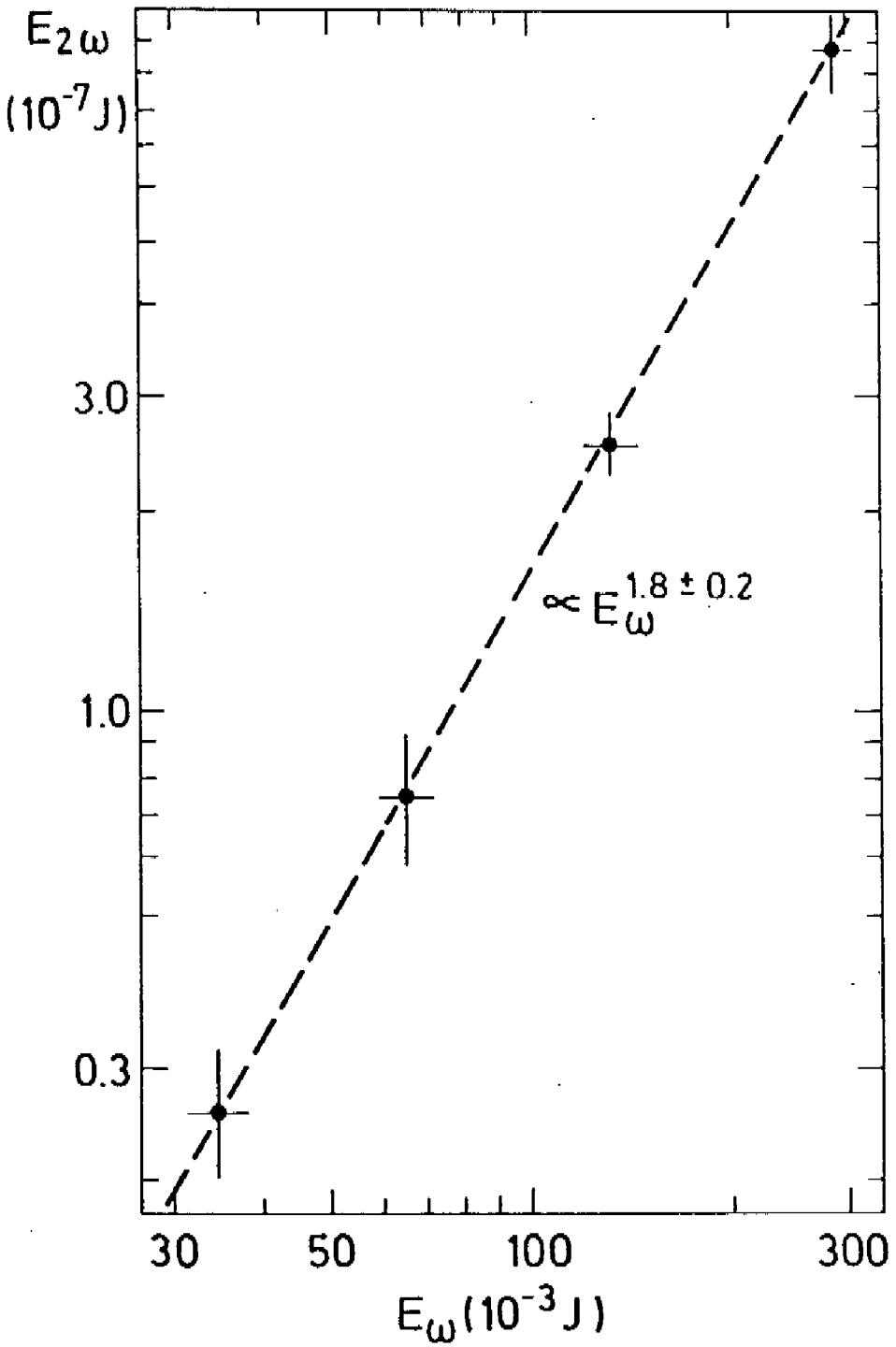
$E_{2\omega}$
$(10^{-7}J)$
3.0
1.0
0.3
$\propto E_{\omega}^{1.8 \pm 0.2}$
30
50
100
300
$E_{\omega}(10^{-3}J)$

Fig. 2

Resonance Absorption of a Wavelength-shifted Probe Beam in a Laser-Produced Plasma

A.G.M. Maaswinkel
Projektgruppe für Laserforschung der Max-Planck-Gesellschaft zur Förderung der Wissenschaften e.V.
D-8046 Garching bei München
Federal Republic of Germany

Abstract

We investigated resonance absorption of a weak probe beam in a plasma produced by 0.53 µm laser irradiation of planar targets at 10^{14} W/cm^2. The probe beam (λ = 1.06 µm) could be delayed in time relative to the 0.53 µm pulse. Thus we found a shift of the resonance absorption maximum towards smaller angles of incidence for increasing time delays. This is expected on account of the hydrodynamic expansion.

The absorption of intense laser radiation in dense hot plasmas is a central problem in laser fusion experiments. Of particular interest is resonance absorption since it is independent of intensity and wavelength of the laser, and is effective even in a collisionless plasma. Resonance absorption has been observed at a number of wavelengths: at 1.06 μm /1-2/ and 0.53 μm /2/, and more recently at 0.26 μm /3/ and 10.6 μm /4/. A common feature of all these experiments was that maximum absorption occurred for angles of incidence between 20° - 30°. According to the theory /5/ this corresponds to a scale length L at the critical density of one vacuum wavelength, $L \approx \lambda_o$. It is generally believed that such a steep density gradient results from profile steepening by radiation pressure. This implies that resonance absorption at high intensities is complicated by other processes occurring simultaneously.

In order to isolate the basic mechanisms it is therefore highly desirable to investigate resonance absorption under less complex conditions. In this paper we report for the first time an experiment where plasma production and heating has been separated from the investigation of the resonance absorption process. For this purpose we have investigated the angular dependence of a weak, wavelength shifted (1.06 μm) probe beam in the plasma formed by an intense laser beam (0.53 μm). In this manner we can not only eliminate high intensity effects but also the absorption mechanism under investigation takes place in an (underdense) region of the plasma which is presumably less complicated than the critical density region of the main laser itself. In addition we could delay the probe pulse relative to the main laser pulse and observe the influence of the changing plasma gradient on the angular dependence of resonance absorption.

We produced the plasma with a 0.53 μm wavelength laser beam of intensity 1 - 3×10^{14} W/cm^2. The pulse duration was 30 ps. On the same axis a weak probe beam of wavelength 1.06 μm and 30 ps duration was focussed, with an intensity of 5×10^{10} W/cm^2. At this intensity no effects due to radiation pressure and only negligible heating would be expected. The probe pulse could be delayed in time relative to the main pulse up to 100 ps.

The experimental set-up is shown in Fig. 1. The 1.06 μm laser beam is converted in a KDP type II crystal with a conversion efficiency of 35 %. The 0.53 μm light is isolated with a BG 18 filter, and it is focussed onto target with an f/20, 400 mm focal length achromatic lens to a spot of 80 μm diameter. The average intensity is 1 - 3 x 10^{14} W/cm^2. The polarization of the beam is 45° to the plane of incidence. After the KDP II crystal 4 % of the light is separated by a beam splitter. It is directed along the same axis as the plasma producing beam by a mirror, which can be translated axially to adjust the time delay $\Delta\tau$. The beam is then attenuated by a factor 200. The polarization of the 1.06 μm beam is turned to s or p with a $\lambda/2$ plate and the 1.06 μm beam is transmitted through a mirror, which is a 100 % reflector for the 0.53 μm beam. It is then focussed with the same lens to a spot of approximately 80 μm. During the experiment great care was taken that both beams were parallel, with a divergence less than 30 μrad; therefore both foci overlapped with at maximum 10 μm distance between the two centers. The time delay between the 0.53 μm and 1.06 μm pulse was verified by a streak camera of 10 ps resolution.

The angle of incidence was varied between 6° and 60° by rotating the target. As target material we used copper coated mirrors of optical quality. The incident and reflected 1.06 μm energy was measured with p-i-n diodes covered with

diffusors and with RG 645 filters to surpress the 0.53 μm light. The reflected light was collected from a solid angle of 7.10^{-2} Sr; it was verified by additional detectors that outside of this solid angle no significant contribution to the total reflectance occurred (total contribution < 1 %). hence it follows that the plasma layer reflecting the probe beam may be considered as smooth, and that the measured reflectance equals the total reflectance. Calibration of the detector R_{SPEC} was done in situ by firing only 1.06 μm light onto the target (no plasma is produced by the weak probe beam) and measuring the ratio of the detector signals This defined 100 % reflectance, since the reflectivity of the Cu-target was measured to be $\geq$ 98 % for 1.06 μm.

During experiments we checked that the probe beam was reflected from the plasma, and not from the copper surface. For this purpose the highly reflecting copper target was replaced by a glass target, whose reflectivity for the probe beam alone was only 8 %. Upon irradiation with the 0.53 μm beam this target showed the much higher plasma reflectance (up to 70 %, see Fig. 2) for the probe beam, identical to that measured for the plasma produced on the copper target.

For the particular choice of the wavelength of the probe beam (interacting with the plasma at one quarter of the critical density N_{cr} of the main laser beam) one might fear complications if the $2\omega_{pe}$ instability would be excited at $N_{cr}/4$ by the main laser beam. Since excitation of this instability should result in $3/2\,\omega_L$ emission, we have checked carefully the emission of $\lambda = 0.355$ μm radiation from the plasma. Within the sensitivity of the spectrograph it was not detectable ($E_{0.355\mu m}/E_{0.53\mu m} < 10^{-8}$). Therefore we presume that the instability is not excited in our parameter regime (from /6/ the threshold for $\lambda = 0.53$ μm, $L = 1$ μm, $T_e = 0.5$ keV is estimated at $I = 2 \times 10^{15}$ W/cm^2, which is well above our irradiance level).

The experimental results are plotted in Fig. 2; the data points are averaged over approximately 10 shots. For different time delays, $\Delta\tau$ = 15,55 and 70 ps between the maxima of the two pulses, the reflectance of the 1.06 µm light was measured for angles of incidence between 6° and 60° (left curves). In the limit of normal incidence ($\vartheta = 0°$) the plane of incidence is not defined, and one cannot distinguish between s- and p-polarization; therefore the reflectance should be identical ($R^s = R^p$), which we have verified explicitly for $\Delta\tau$ = 55 ps. For all time delays a clear difference between R^s and R^p is visible for oblique incidence. We attribute this to resonance absorption: to isolate its contribution we have formed the ratio $(R^s - R^p)/R^s$ in the right hand graphs, and fitted it with the theoretical resonance curve taken from /7/. From the fit a value for the density scale length at the critical density (for 1.06 µm) can be estimated: for $\Delta\tau$ = 15 ps an angle of maximum absorption of $\vartheta_m = 22°$ is obtained giving a scale length of L = 0.8 µm. At $\Delta\tau$ = 55 ps maximum absorption is found at $\vartheta_m \approx 12°$ from which L ≈ 4 µm is concluded. At $\Delta\tau$ = 70 ps the maximum value of $(R^s - R^p)/R^s$ was measured at $\vartheta = 6°$. The measured data no longer allows a definite determination of the angle of maximum resonance absorption, but an approximate fit shown in Fig. 2 corresponds to $\vartheta_m = 9°$ with a scale length of L = 16 µm. We have also made a set of measurements with time delay $\Delta\tau$ = 100 ps; here the shot-to-shot variation in R^s and R^p was very large, and no reproducable difference between them was obtainable. This fact is also visible in Fig. 2, where the error bars in $(R^s - R^p)/R^s$ increase for large time delays. The reason for this phenomenon is not clear at this moment, it must be due to the irreproducability of the plasma conditions at long times after the heating pulse.

From Fig. 2 we see that for $\Delta\tau$ = 15 ps the experimental points for $(R^s - R^p)/R^s$ can be fitted excellently by the theoretical curve for resonance absorption. This good agreement suggests that in this experiment the probe beam is reflected from a smooth plasma. The steep density gradient of 0.8 µm, obtained from the theoretical fit, is probably not produced by radiation pressure, which should be negligible for the probe beam; rather the steep gradient is simply the result of the limited plasma expansion in 15 ps. Secondly we observe for larger time delays a shift of the resonance absorption curve to smaller angles of incidence. This trend is easily seen from the increasing absorption at an angle of incidence of ϑ = 6° with increasing delay time. For $\Delta\tau$ = 15 ps we find $(R^s - R^p)/R^s$ = 0, for 55 ps it amounts to 0.2, and for 70 ps it is 0.4. Thus we have demonstrated that the resonance function does not necessarily have its maximum at 20 - 30°, which was the value found in all past experiments. The theoretical fits in our experiment indicate a scale length L increasing in time; if we model plasma expansion by an isothermal rarefaction wave, the values obtained for L lead to reasonable values for the sound velocity of 1-2 x 10^7 cm/s.

In summary we have investigated resonance absorption in a preconditioned plasma with a probe beam, in the limit of weak intensities and without the complication of previous high intensity experiments. The thus obtained absorption curve confirms the theory for resonance absorption; the observed shift in the absorption curve for increasing time is expected theoretically for plausible plasma conditions.

Acknowledgement

The author is very greatful to Dr. Sigel for his valuable advice during the work, and to Mr. Wanka for his support during the experiments.
He acknowledges receipt of a Euratom grant.
This work was supported by the Bundesministerium für Forschung und Technologie and Euratom.

/1/ K.R. Manes, V.C. Rupert, J.M. Auerbach, P. Lee, and J.E. Swain, Phys. Rev. Lett. 39, 281 (1977)

/2/ A.G.M. Maaswinkel, K. Eidmann, and R. Sigel, Phys. Rev. Lett. 42, 1625 (1979)

/3/ A.G.M. Maaswinkel, Opt. Commun. 33, 62 (1980)

/4/ E. Fabre, J. Virmont, F. Amiranoff, R. Fabbro, C. Garban, and M. Weinfeld, 21st APS Meeting, Division of Plasma Physics, Boston 1979

/5/ V.L. Ginzburg, The Propagation of Electromagnetic Waves in Plasmas (Pergamon, Oxford 1970), p. 267

/6/ M.N. Rosenbluth, Phys. Rev. Lett. 29, 565 (1972)

/7/ H. Kull, Max-Planck-Gesellschaft zur Förderung der Wissenschaften e.V., Report No. PLF 16/1979 (unpublished)

Figure Captions

Fig. 1 Schematic diagram of the probe-beam experiment. The 0.53 μm beam is produced in the KDP II crystal. Its intensity on target is $1\text{-}3\times10^{14}$ W/cm^2. The 1.06 μm probe beam is delayed in time; its intensity is 5×10^{10} W/cm^2.

Fig. 2 Reflectance in 7×10^{-2} Sr as function of the incidence angle for s- and p-polarized light and λ = 1.06 μm (left); comparison with theory from ref. 7 (right). Curves are for time delay $\Delta\tau$ = 15,55 and 70 ps.

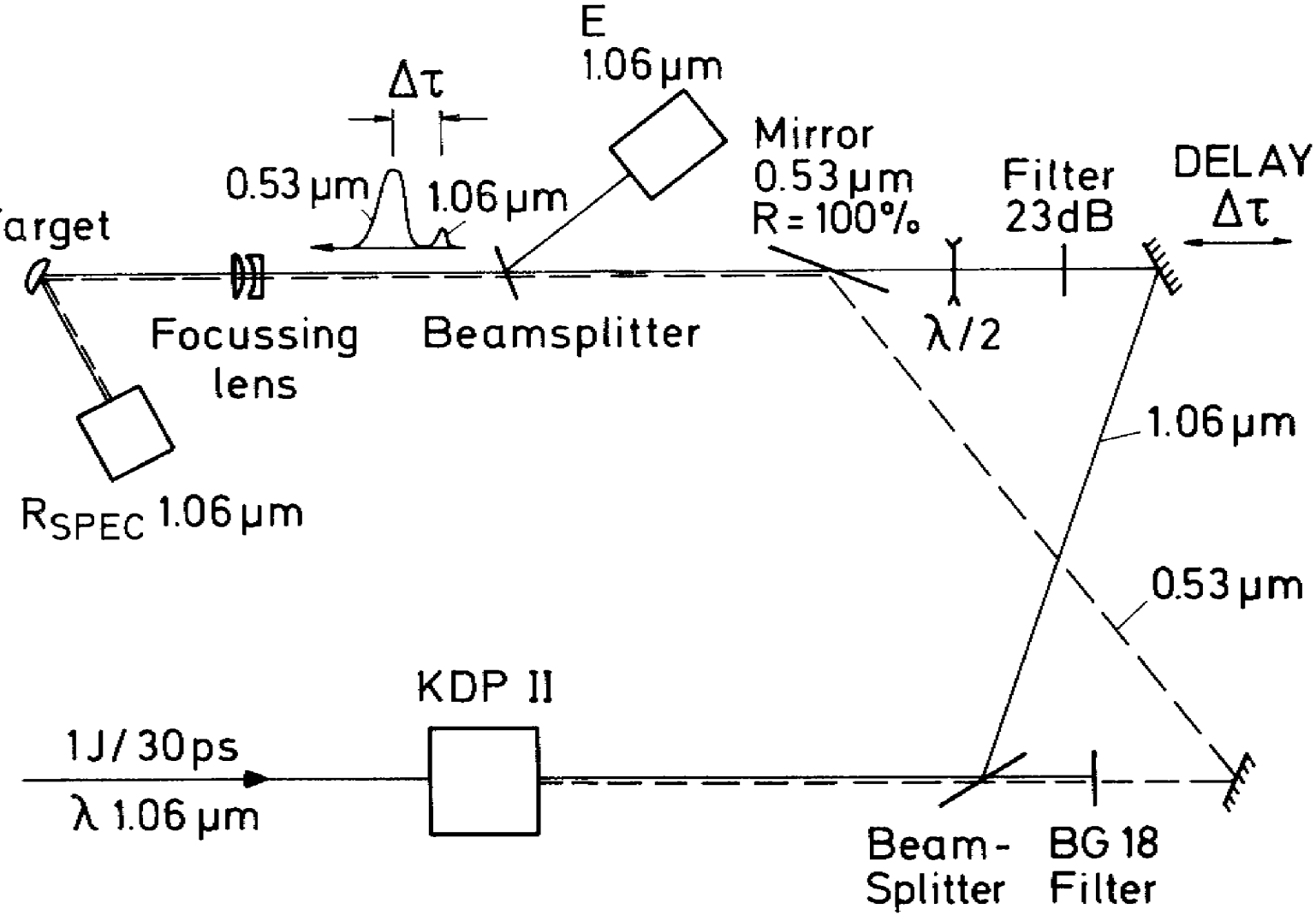
E
1.06 µm
Δτ
Mirror
0.53 µm
R = 100%
Filter
23dB
DELAY
Δτ
0.53 µm
1.06 µm
Target
Focussing
lens
Beamsplitter
λ/2
1.06 µm
R SPEC 1.06 µm
0.53 µm
KDP II
1J/30ps
λ 1.06 µm
Beam-
Splitter
BG 18
Filter

FIG. 1

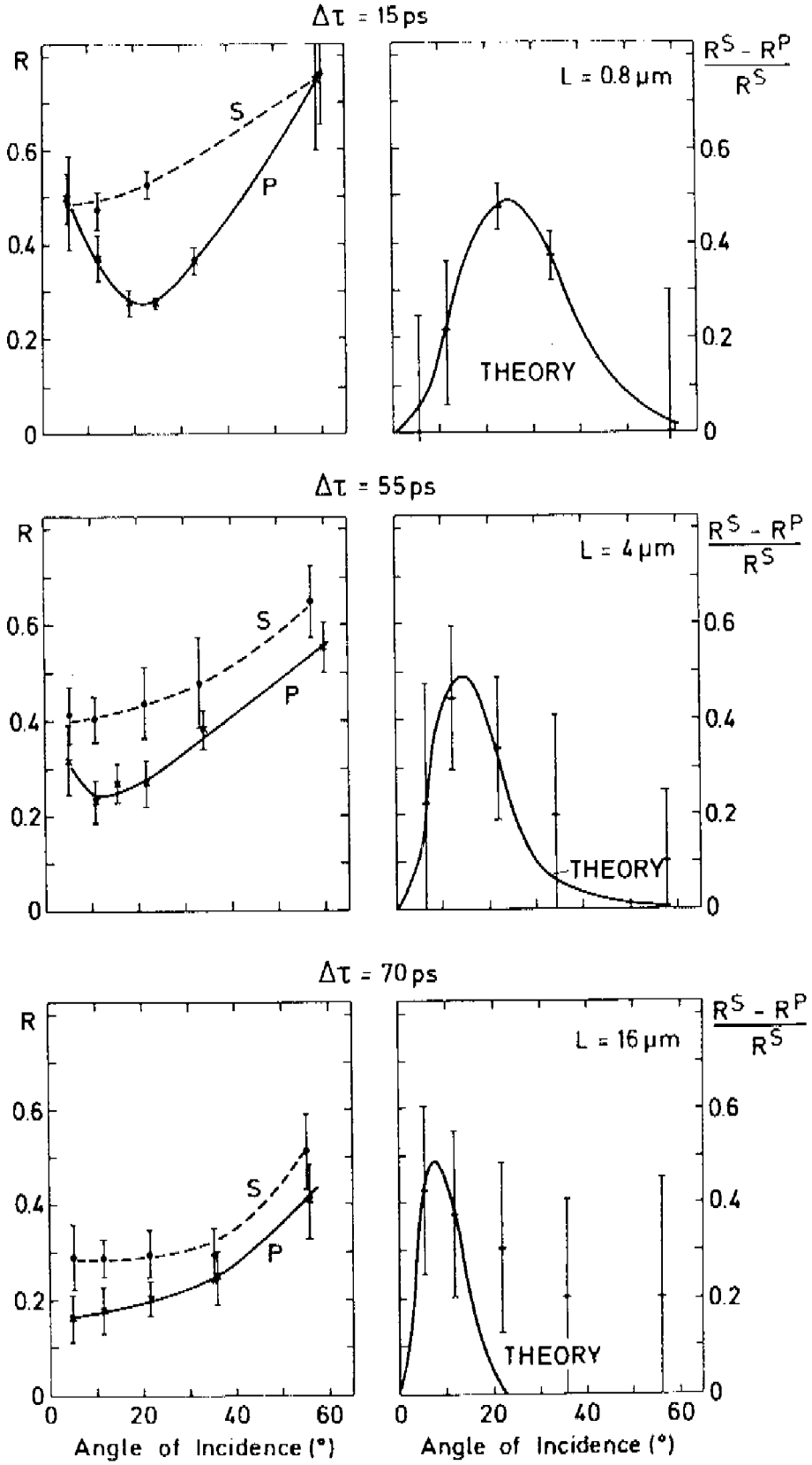
Δτ = 15ps
R
S
P
0.6
0.4
0.2
0
L = 0.8 μm
$\frac{R^S - R^P}{R^S}$
THEORY
Δτ = 55ps
L = 4 μm
Δτ = 70ps
L = 16 μm
0
20
40
60
Angle of Incidence (°)

Fig. 2

V.DISCUSSION

§ 5.1 EXPANSION OF THE PLASMA

In the experiments described in chapter IV the absorption mechanism of linear mode conversion was isolated; from the angle of incidence where maximum absorption occurred we could derive a value of the density scale length at the critical density. In the present section we want to compare this scale length with the one obtained by a simple model of a plasma expanding into vacuum; it is described by a plane isothermal rarefaction wave propagating into the plasma /1 - 3/.

In the model it is assumed that the ions are cold ($T_i = 0$), and that the electrons are in isothermal equilibrium with temperature T_e (infinite heat conductivity). The plasma is assumed to be quasi-neutral: $N_e = Z N_i$. The equation of continuity for the ions is:

$$\frac{\partial N_i}{\partial t} + \frac{\partial}{\partial x}\left(N_i v_i\right) = 0 \qquad (5.1)$$

where v_i is the ion velocity.
The momentum equations for ions and electrons are:

$$N_i M_i \left(\frac{\partial v_i}{\partial t} + v_i \frac{\partial v_i}{\partial x}\right) = Z e N_i E \qquad (5.2a)$$

$$N_e m_e \left(\frac{\partial v_e}{\partial t} + v_e \frac{\partial v_e}{\partial x}\right) = - e N_e E - \frac{\partial p_e}{\partial x} \qquad (5.2b)$$

with $p_e = N_e k_B T_e$. We neglect the inertia term in the electron momentum equation, which means that high frequency plasma oscillations are neglected. Then from eq. (5.2b) it follows by writing the electric field as the gradient of a potential, $E = - \partial \Phi / \partial x$:

$$\frac{1}{N_e}\frac{\partial N_e}{\partial x} = \frac{e \Phi}{k_B T_e}$$, which gives the Boltzmann relation:

$$N_e = Z N_0 \exp\left(\frac{e \Phi}{k_B T_e}\right) \qquad (5.3)$$

By addition of eq. (5.2a) and (5.2b) we obtain then:

$$\frac{\partial v_i}{\partial t} + v_i \frac{\partial v_i}{\partial x} = -\frac{1}{M_i N_i} \frac{\partial p_e}{\partial x} =$$

$$-\frac{1}{M_i N_i} \frac{\partial p_e}{\partial N_i} \frac{\partial N_i}{\partial x} = -c_s^2 \frac{1}{N_i} \frac{\partial N_i}{\partial x} \qquad (5.4)$$

here $c_s = \left\{ \frac{1}{M_i} \frac{\partial p_e}{\partial N_i} \right\}^{1/2} = \left\{ \frac{Z k_B T_e}{M_i} \right\}^{1/2}$ is the ion sound velocity.

Equations (5.1) and (5.4) can be solved by a similarity solution well known from fluid mechanics /4/. We introduce the self-similar variable $\xi = x/c_s t$ and the normalized quantity $u = v_i/c_s$. The symbol ' stands for $\partial/\partial\xi$ Equations (5.1) and (5.4) may then be written:

$$(u - \xi) N_i' + N_i u' = 0 \qquad (5.5)$$

$$(u - \xi) u' + N_i'/N_i = 0 \qquad (5.6)$$

Elimination of N_i' and u' gives the solution $(u - \xi)^2 = 1$, from which $v_i = x/t \pm c_s$ follows. If the plasma at $t < 0$ is restricted to the region $x > 0$ with ion density $N_i = N_0$ it will expand into the region $x < 0$ for $t > 0$; the rarefaction wave will propagate into the undisturbed plasma with velocity c_s. The ion velocity for $t > 0$ is then

$$v_i = x/t - c_s \qquad (5.7)$$

The ion density profile is found by substituting solution (5.7) in eq. (5.6), and has the form:

$$N_i = N_0 \exp\left(\frac{x}{c_s t} - 1\right) \qquad (5.8)$$

See Fig. 5.1. The electron density profile has the same dependence on x/t .

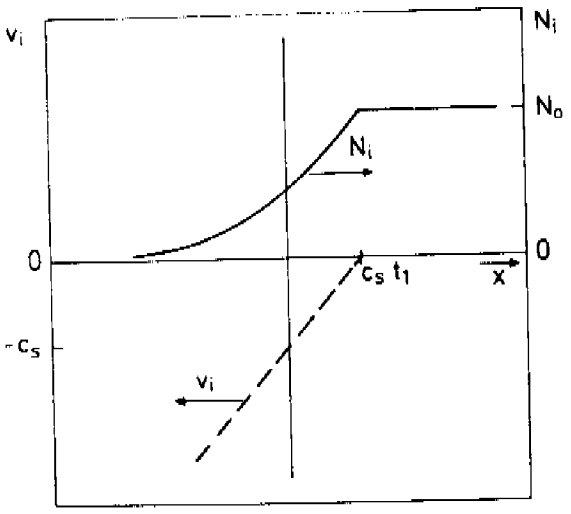

Fig. 5.1 Ion density profile $N_i(x, t_1)$ and velocity profile $v_i(x, t_1)$ for a plane isothermal rarefaction wave at $t = t_1$.

The density scale length at the critical density was defined in chapter II under eq. (2.21) as

$$L = \left\{ \frac{1}{N_e} \frac{dN_e}{dx} \right\}^{-1}_{N_{cr}} \qquad (5.9)$$

For the exponential density profile (5.8) the scale length has the value $L = c_s t$ (5.10)

In the following sections we shall use the formulas (5.8) and (5.10) for the interpretation of the experimental results.

§ 5.2 COMPARISON OF THE RESULTS WITH COLLISIONAL ASORPTION

Upon interpretation of the experimental results by theoretical models for absorption it should be stressed that it may be doubtful whether one can interprete these results in a unique way, since the absorption in the highly inhomogeneous and rapidly expanding plasma depends on various parameters: the amount of collisional absorption depends on the electron-ion frequency, which is a function of T_e, N_e and Z, and on the penetration depth of the light wave into the plasma (a function of the angle of incidence and of the specific electron density profile).

Linear mode conversion occurring for P-polarized light has a maximum absorption for an angle of incidence depending on the density scale length; in addition linear mode conversion can also occur for S-polarization. If the critical density layer is rippled so that a fraction of the incident S-polarized light has a component parallel to the local density gradient, its polarization is changed into "P". Finally the density profile of the plasma will change during the plasma expansion. Thus the actual situation is very complex, even under the assumption that only these two absorption mechanisms are present.

We assume that in case of S-polarization collisional absorption is the determining absorption mechanism and we neglect for the moment that linear mode conversion may be responsible for a (minor) fraction of absorption in case of rippling.

In case of collisional absorption the reflectance can be described by the formula $R_{TOT} = \exp(-\alpha \cos^{\beta}\vartheta)$ (5.11); this is the same form as formulas (2.32) and (2.33). Here the coefficient α determines the reflectance at normal incidence ($\vartheta_o = 0°$) and is given by $\alpha = \alpha_o k L A$, where α_o is a constant depending on the density profile (linear profile $\alpha_o = 32/15$,exponential profile $\alpha_o = 8/3$), A is the normalized collision frequency $A = (\nu_{ei})_{Ncr}/\omega$. The factor β determines the decrease in collisional absorption for increasing angles of incidence (with lower cut-off density) and was found to be $\beta = 5$ for a linear density profile and $\beta = 3$ for an exponential profile.

We have tried to interpret the reflectance obtained for S-polarized light in terms of inverse bremsstrahlung. We have investigated the wavelengths 1.06 µm, 0.53 µm and 0.26 µm. The data are collected from measurements with short (30 ps) laser pulses at intensity 4×10^{13} - 3×10^{14} W/cm^2, with focal spot of 40 µm diameter, and from measurements at

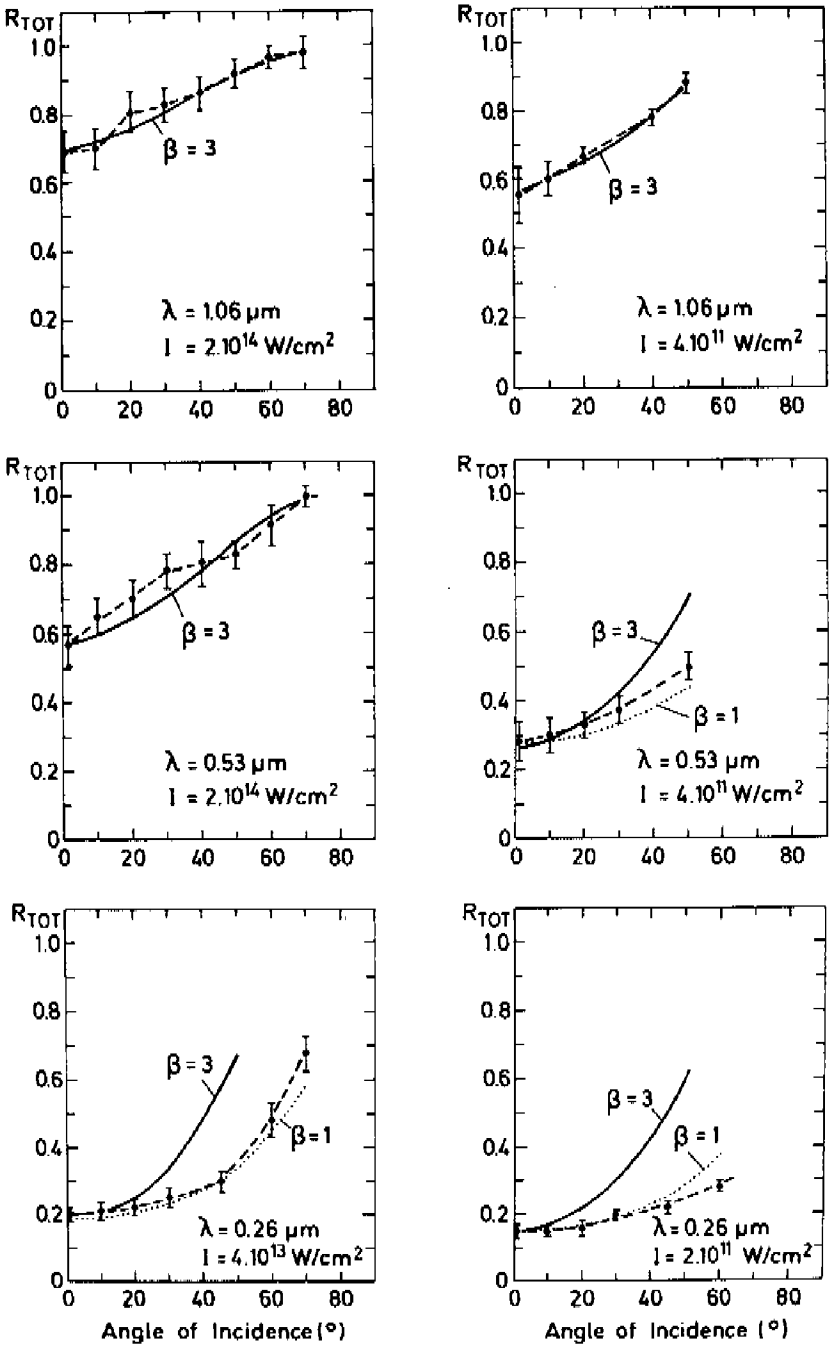

Fig. 5.2 Reflectance into 4π sr for S-polarized light and τ = 30 ps (dashed curves). Best fits obtained with formula (5.11) for β = 3 (solid curves) and β = 1 (dotted curves).

$2 - 6 \times 10^{11}$ W/cm^2 with focal spot of 400 - 1000 µm diameter. The reflectance R_{TOT} is determined from measurements with the Ulbricht sphere, and is therefore the reflectance into 4π sr.

The experimental results presented in Fig. 5.2 are partially taken from /5/ and from § 4.1 and § 4.2. We fit the experimental (dashed) curves with a curve of the form (5.11), where the coefficients α and β are fitting parameters. The constants α are determined by the reflectance at normal incidence. They correspond to physical parameters (λ, L, T_e, Z) which for the fits from Fig. 5.2 are listed in Table 5.3. The parameters L, T_e, Z are arbitrary as long as their combination gives the right value of α. We have taken values for them which are supported by other data: the values for the density scale length L are deduced from the angle of maximum resonance absorption in case of P-polarization. The values for the electron temperature are taken from x-ray measurements published by other groups /6 - 8/. Z, the averaged charge state, is estimated from the electron temperature: in short pulse experiments the time-dependence of the ionization is important /9/ and has to be taken into account.

λ (µm)	I (W/cm^2)	$R_{TOT}(0°)$	L (µm)	T_e (eV)	Z
1.06	2.10^{14}	0.69	1.0	350	12
1.06	4.10^{11}	0.55	0.4	100	10
0.53	2.10^{14}	0.56	0.5	400	12
0.53	4.10^{11}	0.28	0.2	100	10
0.26	4.10^{13}	0.20	0.2	200	10
0.26	2.10^{11}	0.15	0.1	100	8

Table 5.3: Combination of parameters λ, L, T_e, Z for which the required collisional absorption at normal in Fig. 5.2 is obtained.

REFLECTANCE AT NORMAL INCIDENCE

Upon comparison of the reflectance in dependence of wavelength and intensity we readily see that the absorption at shorter wavelength is larger. This fact supports the supposition of inverse bremsstrahlung as the responsible absorption mechanism because it is more effective at shorter wavelengths. This can be seen from formula (5.11). If we take the product kL as constant for all three wavelengths (this follows from interpretation of the data for P-polarization: see § 5.3) then the wavelength dependence is given by the normalized collision frequency $A = (\nu_{ei})_{N_{cr}} / \omega$. As ν_{ei} is proportional to N_{cr}, and N_{cr} scales with ω^2, A is proportional to ω, and thus $\alpha \sim \omega$. This means that, as long as α is small, the inverse bremsstrahlung absorption should scale proportional to ω, because it is defined as $f_{ib} = 1 - R_{TOT} = 1 - \exp(-\alpha) \approx \alpha$ From Fig. 5.2 we see that this scaling is approximately fulfilled at intensity 10^{14} W/cm^2 (absorption for 1.06 μm, 0.53 μm and 0.26 μm is 0.31, 0.45 and 0.80 respectively). It will be clear that this argument oversimplifies the reality, since we neglect changes in T_e and Z. At intensity 10^{11} W/cm^2 the electron temperature is presumably lower, which enhances the absorption ($\nu_{ei} \sim T_e^{-3/2}$). The data show the parameter regime where collisional absorption is effective: short wavelengths and moderate intensities.

REFLECTANCE AT OBLIQUE INCIDENCE

The dependence of collisional absorption on the angle of incidence is contained in the factor β in formula (5.11). With the choice of an exponential profile (corresponding to isothermal expansion), for which $\beta = 3$, a good agreement is obtained for the wavelengths 1.06 μm and 0.53 μm (Fig. 5.2). For 0.26 μm wavelength we observe that for large angles of incidence the estimated reflectance is higher than the

actual one. Apparently the exponential density profile, derived from the isothermal expansion, does not apply. The other "extremum" in case of an expanding plasma occurs if the heat conductivity is negligible; as the classical (Spitzer) heat conductivity coefficient scales with $T_e^{5/2}$, this is expected to occur in cold plasmas. In this case, of adiabatic expansion, the electron temperature and density are related by T_e/N_e^2 = constant. If this relation is used to calculate the collisional absorption for oblique incidence (following the method from § 2.2) a value for the coefficient $\beta = 1$ is found. We have drawn the curves with $R_{TOT} = exp(-\alpha \cos\vartheta)$ in Fig. 5.2 for $\lambda = 0.26$ μm; indeed a better agreement is found than with $\beta = 3$. We remark that also in case of low intensity (4×10^{11} W/cm^2) at wavelength 0.53 μm the curve with $\beta = 1$ has approximately the right shape. We notice that it is not possible to fit the angular dependence with $\beta = 5$, which corresponds to a linear density profile: for oblique incidence this profile gives values for the reflectance which are much higher than the experimental values, for all conditions in Fig. 5.2: e.g. for $\lambda = 0.53$ μm and $I = 2 \times 10^{14}$ W/cm^2 the reflectance for $\vartheta = 50°$ predicted by this model is $R_{TOT} = 0.94$, whereas the experimental value is 0.80.

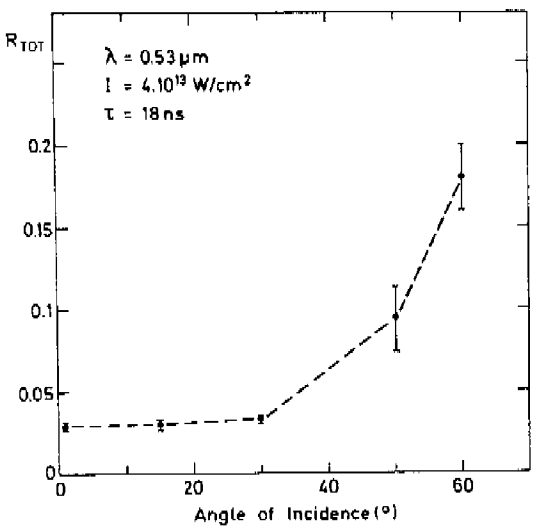

Fig. 5.4 Reflectance into 4π sr for S-polarized light; $\lambda = 0.53$ μm and $\tau = 18$ ns. Notice the different scale of the y-axis compared to Fig. 5.2.

In addition we present in Fig. 5.4 the total reflectance as function of angle of incidence for long (18 ns) pulses at wavelength 0.53 μm and S-polarization. The incident energy is 0.8 J, the focal spot diameter 10 μm, resulting in averaged intensity of 4×10^{13} W/cm^2. We see that for these long pulses and wavelength 0.53 μm the absorption is very effective, larger than 95 %. We believe that the mechanism is again collisional absorption. The density scale length at these long pulses may be very large; its value may be determined by the focal spot radius (5 μm) or by the scale length of the isothermally expanding plasma ($\approx$ 100 μm). The extended underdense plasma results in an absorption, which is effective even for large angles of incidence. In this case, however, the angle of incidence is not well defined, because the plasma expands spherically. It is therefore not possible to compare the experimental curve with formula (5.11) which is derived for planar geometry. The reflectance for a spherically expanding plasma is calculated in /10/ as $R_{TOT} = exp(-\frac{\pi}{2} k L A)$. For $\lambda = 0.53$ μm, $L \geq 5$ μm, $T_e = 200$ eV and $Z = 10$ this gives very low reflectances $R_{TOT} \leq 0.03$ in approximate agreement with Fig. 5.4.

In conclusion we find that in case of S-polarization a comparison of the experimental curves with collisional absorption shows that a good fit can be obtained for a plausible choice of plasma parameters. On the other hand it is clear from the discussion that a change in the (only approximately known) plasma parameters causes a change in the absorption coefficient approximately proportional to it; one should therefore be careful to predict absorption by inverse bremsstrahlung too quantitatively. The data in Fig. (5.2) and (5.4) indicate that effective collisional absorption occurs for short wavelengths, moderate intensities and long pulses.

§ 5.3 COMPARISON OF THE RESULTS WITH LINEAR MODE CONVERSION

We briefly recall the properties of linear mode conversion, as derived in § 2.3:

- Linear mode conversion or resonance absorption occurs in laser-produced plasmas if the electric field of the incident wave has a component parallel to the electron density gradient ∇N_e (P-polarization);
- it reaches a maximum absorption of ≈ 0.5 for an optimum angle of incidence given by $(kL)^{2/3} \sin^2 \vartheta_m \approx 0.5$ (5.12) (see Fig. 2.4).
- it is accompagnied by second harmonic emission, which has its maximum at the same angle ϑ_m.
- linear mode conversion is a linear absorption process and is independent of wavelength and intensity.

INTERPRETATION OF THE DENSITY SCALE LENGTHS

In the letters in § 4.1 and § 4.2 we have isolated the contribution of resonance absorption (f_{ra}) by forming the ratio

$$f_{ra} = (R^S_{SPEC} - R^P_{SPEC}) / R^S_{SPEC} \qquad (5.13).$$

This can be derived by a simple argument. The total reflectance R_{TOT} is composed of the specular reflectance R_{SPEC} and diffuse reflectance R_{DIFF}; the latter has been observed to be independent of the polarization of the beam (§ 4.1). Therefore the effect of resonance absorption is expected to be visible in the specular beam, and to occur only for P-polarization, R^P_{SPEC}. We assume that the only other effective mechanism present is inverse bremsstrahlung with a reflectance R_{ib}, effective for both polarizations S and P. We can then write the specular reflectances as

$$R^S_{SPEC} = R_{ib}$$
$$R^P_{SPEC} = R_{ib}\,(1 - f_{ra})$$

By elimination of R_{ib} the relation (5.13) is found.

Upon evaluation of the curves for f_{ra} in § 4.1 and § 4.2 for intensities 4 x 10^{13} - 2 x 10^{14} W/cm^2 the maximum of f_{ra} has been found at an angle ϑ_m = 20 - 22°; the same angle of 20° has been found for the maximum of 2ω emission in letter § 4.3. This corresponds according to eq. (5.8) to a density scale length L of about one vacuum wavelength, for all three wavelengths considered. We can compare this value of L with the scale length ℓ determined by the expanding plasma during the laser pulse; this length is $\ell = c_s\tau$ (5.10), where τ is the laser pulse duration and c_s the sound velocity (eq. (5.4)) . For parameters T_e and Z taken from Table 5.3 and a Cu-plasma we find values for c_s between 5 x 10^6 - 10^7 cm/s. This gives in 30 ps ℓ = 1.5 - 3 µm (for UV experiments the laser pulse is estimated 20 ps, which gives $\ell \approx$ 1 µm). These values for ℓ are larger than those obtained from evaluation of the resonance curve, but agree within a factor of three. For the experiments made at 2 - 6 x 10^{11} W/cm^2 the maximum of the resonance curve is located at $\vartheta_m \approx 30°$, which gives a value for the scale length of about 0.4 (for all three wavelengths); the tendency is clear: caused by the lower irradiation level the electron temperature will be lower, and hence the sound velocity c_s will be smaller ($\approx$ 2 x 10^6 cm/s.) Then the scale length, determined by the hydrodynamic expansion, will be smaller, too.

In § 4.4 we have found that a probe pulse interacting with the plasma produced by the main laser at increasing time delays has its angle of maximum absorption at decreasing values of ϑ ; this is also interpreted as increase of the density scale length. For quantitative interpretation there are some limitations. The width of the main laser and probe pulse (30 ps) limit the time resolution (the delays are 15 - 70 ps). Further it can be seen from relation (5.12) that for maximum absorption at small angles ϑ a small uncertainty in the value of ϑ has a large effect on the value of L because $L \sim \vartheta^3$. In Fig. 5.5 we have plotted the values for L, obtained from Fig. 2 in § 4.4, in de-

pendence of time delay $\Delta\tau$. We obtain values for the sound velocity $c_s = L/\Delta\tau$ between 1 and 1.8 x 10^7 cm/s, in approximate agreement with our earlier results.

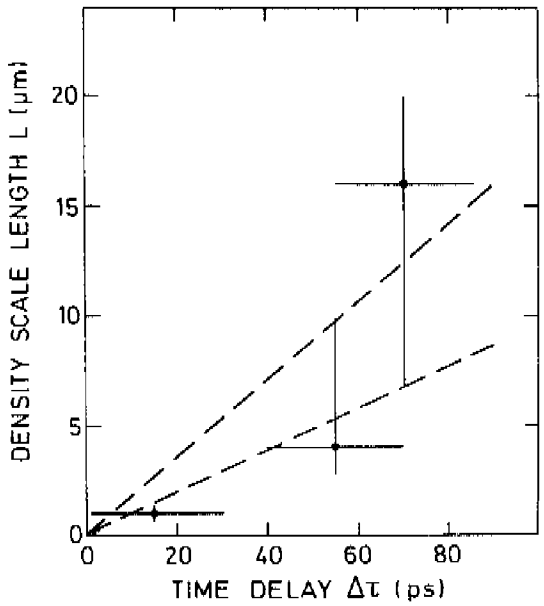

Fig. 5.5 Density scale length L at increasing time delays $\Delta\tau$ between the probe pulse and the main laser pulse (from § 4.4). The two dashed lines give l for the sound velocities c_s = 1 and 1.8x10^7 m/s.

In the paper from § 4.1 it has been remarked that the experimental curve for resonance absorption deviates from the theoretical curve for large angles of incidence, a behaviour which has also been observed in other short-pulse reflectance measurements /8, 11/. Now we can interpret this phenomena on base of Fig. 5.5. At the beginning of the plasma expansion the density scale length is very small (< 1 µm) and the corresponding angle of maximum absorption is rather large. During the laser pulse the plasma expands, and L increases to approximately one vacuum wavelengh in 30 ps. The angle of maximum resonance absorption shifts to smaller values. The observed deviation of the experimental curve is then due to this transient phenomenon.

THE EFFECT OF A RIPPLED SURFACE ON RESONANCE ABSORPTION

In § 5.2 we have already touched upon the phenomenon that resonance absorption may occur for normally incident light and for S-polarized light in case of a plasma profile which is rippled at the critical density. The presence of diffuse reflectance, independent of the polarization of the light and at normal incidence, as reported in § 4.1, leads to the conclusion that resonance absorption should occur in this case. In fact it has been observed by Balmer et al. /8/ and by Godwin et al. /12/ that the difference in reflectance between S and P-polarization disappears in case of rough target surfaces or very small focal spots. Rippling of the critical density surface may for instance be caused by intensity fluctuations in the laser beam, or by hydrodynamic instabilities. The description of resonance absorption in case of a rippled density profile is generally very complicated, because the electron density is a function of the three coordinates (x, y, z). A separation of the wave equation into components (S and P-polarization) is generally impossible.

We can, however, get an idea of the influence of rippling on the fraction of resonance absorption by a simple model, which has been proposed by Thomson et al /13/. In this model it is assumed that the characteristic length of a ripple is much larger than the laser wavelength, and that we can therefore consider the critical density layer locally as planar. We now follow every incident ray individually; the incident ray is in the yz-plane at an angle ϑ and the critical density is now tilted at an angle Φ . If the tilt of the critical density (originally in the xy-plane) is in the yz-plane (rotation around the x-axis) then the angle ϑ changes to $\vartheta' = \vartheta + \Phi$.

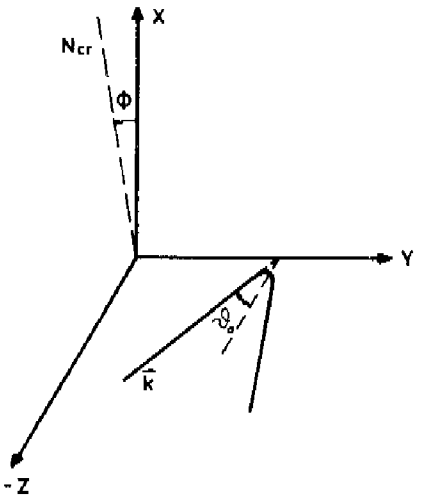

Fig. 5.6 Schematic representation of the effect of rippling. The critical density layer, originally in the xy-plane, is now tilted at angle ϕ ; the $\vec{k}$-vector is incident in the yz-plane.

If the rotation is around the y-axis (Fig. 5.6) the ray changes its polarization: S-polarization will change partially into P and vice versa; the density gradient ∇N_e will change as $\nabla N_e' = (-\sin\phi, 0, \cos\phi)\,\nabla N_e$. We can now perform a coordinate transform, by choosing a new z-axis parallel to $\nabla N_e'$. Further we can choose the $y'z'$ -plane as the new plane of incidence, defined by $\vec{k}$ and $\nabla N_e'$. The new angle of incidence is then given by the inproduct $(\vec{k}, \nabla N_e') = \cos\vartheta' = \cos\phi\cos\vartheta$. We can now construct an orthonormal coordinate system in which the electric field vector can be resolved in a component in the new plane of incidence ("P") and one normally to it ("S"). If we assume that the rippling is stochastic, and ϕ is uniformly distributed between $-\phi_{max}$ and $+\phi_{max}$, with equal probability in the yz-plane and the xz plane then the fraction of the incident light which changes its polarization is /13/

$$f = \frac{1}{2}\,\frac{\sin^2\phi}{\sin^2\vartheta + \cos^2\vartheta\,\sin^2\phi} \qquad (5.14)$$

We have used expression (5.14) to compute the effect of rippling on the fraction of resonance absorption for a specified angle of incidence ϑ_o, and a uniformly distributed random angle ϕ . In Fig. 5.7 the result is

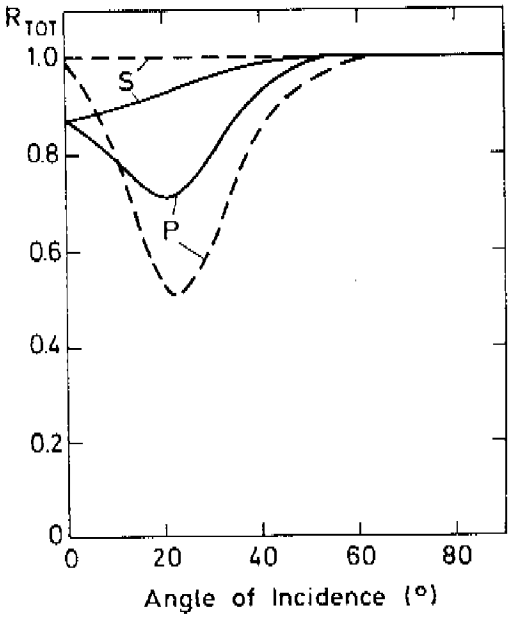

Fig. 5.7 Reflectance from a plasma with rippled critical density layer, $\phi_{max} = 40°$ (solid curves) and from a plasma with a smooth layer (dashed curves). $L = \lambda = 1.06$ µm Resonance absorption is exhibited, collisional absorption is zero.

given for a S- and a P-polarized wave in case where the collisional absorption is equal zero (solid curve); the relevant parameters are $\lambda = L = 1.06$ µm and $\phi_{max} = 40°$. The reflectance in case without rippling is drawn for comparison in the dashed curves. Two effects are readily noticed: first there is absorption for normally incident light ($\vartheta_o = 0°$), amounting to 12 %. Secondly we observe that maximum resonance absorption for P-polarization is now smaller than 50 %, and shifts to a smaller angle of incidence.

It is tempting to use this absorption mechanism for interpretation of the experimental curves, e.g. the curves for S- and P- polarization from § 4.1, since from these measurements we know that there is a considerable amount of diffusely scattered light. We notice also from Fig. 1 in § 4.1 that at $\lambda = 1.06$ µm the maximum difference between R^S_{TOT} and R^P_{TOT} is only 20 %. We have therefore tried to fit the curve at 1.06 µm with a model, where absorption takes place by inverse bremsstrahlung and resonance absorption including

a rippled critical density layer. The result is shown in Fig. 5.8, with parameters λ = 1.06 μm, L = 0.7 μm, T_e = 350 eV, Z = 12 and β = 3; the angle ϕ_{max} is set equal to 25°. The agreement for S-polarization is good, for the P-polarization data we observe a deviation for angles of incidence of 50 - 60°, which has been discussed before as resulting from the non stationary plasma expansion. Similar curves are obtained for 0.53 μm and 0.26 μm. Thus we have demonstrated with a simple model that rippling of the critical density layer may considerably affect the absorption in the plasma.

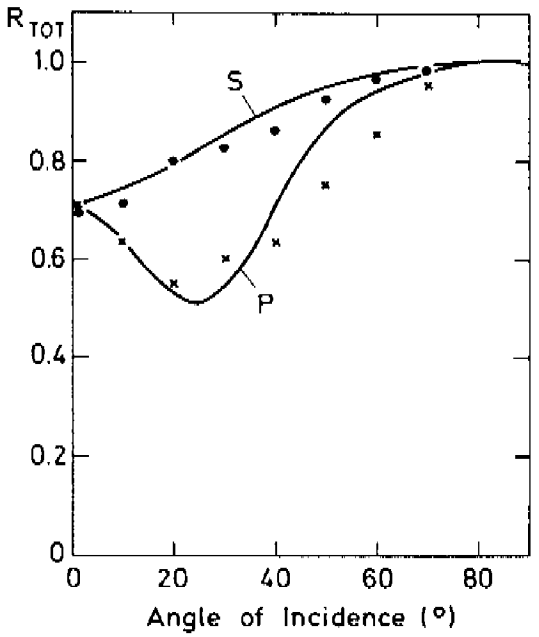

Fig. 5.8 Comparison of the experimentally measured reflectance at 1.06 μm (from § 4.1, Fig. 1) and a theoretical model, including a rippled layer. The dots are S-polarization, the crosses P-polarization data. The error bars, which have been omitted, are ± 7%.

SUMMARY OF THE RESULTS OBTAINED FOR LINEAR MODE CONVERSION

1) linear mode conversion has been isolated from the specular reflectance (§ 4.1 and § 4.2) and behaves as predicted by theory:
   - it occurs for P-polarized light, independent from the the wavelength and intensity, and can be fitted to the theoretical absorption curve.

- it is accompanied by second harmonic emission, which is proportional to the square of the absorption curve (§ 4.3).

2) the density scale length at the critical density found in the experiments is likely to be caused by the expansion of the plasma.
3) the presence of diffusely reflected light makes it probable that resonance absorption is also present for S-polarized light and at normal incidence; this is caused by a rippled critical density layer which may result in 10 - 15 % resonance absorption at normal incidence.

§ 5.4 COMPARISON WITH RESULTS FROM OTHER LABORATORIES

In the analysis of the linear absorption mechanisms, which describe the absorption behaviour of laser-produced plasmas for intensities up to 10^{14} W/cm^2 we refer to recent experimental results from other laboratories.

Concerning linear mode conversion there are now confirmations of this process by several groups. Much experimental evidence, however, is indirect. Moreover the theoretical absorption curve has not been verified by other groups. Direct evidence for linear mode conversion has been obtained at λ = 1.06 µm by Manes et al. /14/ and Godwin et al. /12/, and at 10.6 µm in a recent experiment at Palaiseau /6/. The angle of maximum absorption in these experiments was at 20 - 30° incidence, indicating a density scale length of one vacuum wavelength, the same value as found in our experiments at 1.06 µm, 0.53 µm and 0.26 µm.

The process of inverse bremsstrahlung has lately drawn the attention of several groups, since it may be an efficient absorption mechanism for lasers with long pulses ($\gtrsim$ 1 ns) irradiating targets with high Z materials. This aspect has been investigated by Rosen et al. /15/. For moderate laser

irradiation 3 x 10^{14} W/cm^2 of gold disks (Z = 79) at pulse duration 1 ns they report 50 - 54 % absorption at normal incidence. This amount of absorption is claimed to be due to inverse bremsstrahlung.

Table 5.9 Comparison between the experiments from Palaiseau and Garching. The Palaiseau results are from /6/; the Garching results are from this thesis; the measurements labelled ● are published in /16/. τ is the pulse duration, α is the absorption.

	PALAISEAU			GARCHING		
λ	τ	I W/cm^2	α	τ	I W/cm^2	α
1.06 µm	100 ps	3×10^{14}	30 %	30 ps	3×10^{14}	30 %
		6×10^{11}	48 %		6×10^{11}	42 %
	2.5 ns	10^{14}	45 %	10 ns	10^{14}	48 %
		10^{12}	80 %		● 10^{12}	● 85 %
0.53 µm	80 ps	3×10^{14}	60 %	30 ps	3×10^{14}	43 %
	2 ns	4×10^{13}	80 %	18 ns	4×10^{13}	97 %
0.26 µm	60 ps	$1\text{-}4\times10^{14}$	90 %	20 ps	4×10^{13}	81 %
				150 ps	8×10^{12}	87 %

The absorption as a function of laser wavelength has been investigated (at normal incidence) at the Ecole Polytechnique in Palaiseau. In Table 5.9 we compare some of these results with our experiments. The target material was polyethylene in Palaiseau, in our experiments the target material was Cu or Al/MgF (at 0.26 µm). The results of both groups agree within 10 % for wavelengths 1.06 µm and 0.26 µm; the differences in absorption at 0.53 µm are thought to be due to the different pulse durations. Longer pulses cause a larger density scale length and hence a more efficient collisional absorption. From the table it can be concluded that the absorption increases with shorter wavelengths and with longer pulse durations. These effects are both well described by collisional absorption. Hence it is concluded that under these conditions it is the responsible absorption mechanism.

§ 5.5 PROSPECTS FOR BETTER LIGHT ABSORPTION

From the discussion in § 5.2 it has become clear that the laser light is better absorbed at shorter wavelengths λ, lower irradiance I_{inc} and longer pulse duration τ. This behaviour is consistent with collisional absorption as the responsible mechanism; the scaling of collisional absorption with λ, I_{inc} and τ can be estimated by a simple model /15/. In § 5.2 we have found for moderate absorption by inverse bremsstrahlung

$$f_{ib} = \frac{I_{abs}}{I_{inc}} = 1 - exp(-\alpha) \approx \alpha L A = \frac{2\pi}{\lambda} L \frac{(\nu_{ei})_{N_{cr}}}{\omega}$$

here $(\nu_{ei})_{N_{cr}}$ scales with $Z N_{cr} / T_e^{3/2} \sim Z/\lambda^2 T_e^{3/2}$

If we assume that the density scale length L is determined by the expansion of the plasma, it becomes:

$$L = c_s \tau \sim \left(\frac{Z}{A_o} T_e\right)^{1/2} \tau$$

here A_o is the relative atomic mass.

In case of a hot plasma and long pulses the ratio $\frac{Z}{A_o} \longrightarrow \frac{1}{2}$ (completely stripped ions) and $L \sim T_e^{1/2} \tau$

The collisional absorption I_{abs} scales then as

$$I_{abs} \sim I_{inc} \frac{Z}{\lambda^2} \frac{\tau}{T_e} \qquad (5.15)$$

Now we assume that the absorbed flux is transported by the free streaming heat flux limit, which is for electrons with Maxwellian distribution $I_{abs} = \left(\frac{2}{\pi}\right)^{1/2} v_e N_e k_B T_e$

and scales as $$I_{abs} \sim \frac{T_e^{3/2}}{\lambda^2} \qquad (5.16)$$

By equating (5.15) with (5.16) we can eliminate T_e, and find that the fractional absorption scales as

$$f \sim \frac{T_e^{3/2}}{\lambda^2 I_{inc}} \sim \frac{(Z\tau)^{3/5}}{\lambda^2 I^{2/5}} \qquad (5.17)$$

From this expression we conclude that indeed collisional absorption increases greatly at shorter wavelengths. In addition it will be more effective at longer pulse duration and at lower irradiance. Finally it will increase for higher Z-materials. Although the obtained scaling law (5.17) greatly simplifies the physics, it enables us to extrapolate our experimental results to larger laser systems, which finally have to be used in a laser fusion reactor to obtain a significant yield from irradiation of DT-pellets. A recent study /17/ for requirements on a laser fusion driver gives numbers of required laser energy of 3 - 5 MJ and pulse duration of 5 - 10 ns. For a typical reactor pellet with 0.5 - 1 cm diameter an averaged irradiation level of 10^{14} - 10^{15} W/cm^2 is then obtained.

At this moment we have at our disposal the data from short pulse experiments (30 ps) at intensity $\simeq 10^{14}$ W/cm^2, where the absorption increases significantly by going from wavelength 1.06 µm to 0.26 µm. We have also data from long pulse experiments, where the absorption increases from wavelength 1.06 µm to 0.53 µm (Table 5.9). In addition we remark that the absorption for long (18 ns) pulses at 0.53 µm and intensity 4 x 10^{13} W/cm^2 is larger than for short

pulses. These facts indicate, that the light absorption from the lasers on reactor scale can be very effective, if we can use a laser with short wavelength ($\lambda \lesssim 0.3$ µm) and with sufficiently long pulse ($\tau \gtrsim 1$ ns).

The other absorption mechanism which we have isolated in our experiments is linear mode conversion (resonance absorption). We have shown that it behaves very well in agreement with the theoretical predictions. In particular the maximum absorption is 50 % out of the specular beam. In addition linear mode conversion may be responsible for some absorption ($\approx$ 10 - 15 %) at normal incidence in case of a rippled plasma layer. Resonance absorption is independant of the wavelength of the laser; in this respect it sets no requirements on a laser for fusion purposes. However, as we have mentioned in § 2.3 there are strong indications from the literature that resonance absorption creates supra-thermal ("hot") electrons, which can penetrate into the target and preheat the DT fuel, thus increasing the required energy for efficient compression of the DT gas. There are indications /6/ that the hot-electron temperature for short wavelength irradiation is lower than for longer wavelengths, which would be in favour for short-wavelength lasers. Also we have noticed in § 4.2 that, if collisional absorption is very high, the amount of absorption by linear mode conversion is small (in absolute numbers); in this case the hot electron production should be small, too. We should also mention that for reactor size pellets of several mm thick, preheat may be a less severe problem when the electrons are stopped in the outer layer or shell of the pellet.

In conclusion we can state that we have performed a series of experiments on laser light absorption on planar targets, where we have compared the absorption at wavelengths 1.06 µm, 0.53 µm and 0.26 µm, at intensities $\leqslant 10^{14}$ W/cm^2. A comparison of the experimental results with linear theory has shown that the absorption behaviour is well described by inverse bremsstrahlung and linear mode conversion. This leads to the conclusion that lasers with short wavelengths and ns-pulse duration are attractive for larger systems designed for laser fusion reactors.

References of chapter V:

1. J.E. Allen and J.G. Andrews, J. Plasma Phys. 4, (1970)

2. J. Denavit, Phys. Fluids 22, 1384 (1979)

3. R. Sigel, 20th Scottish Universities Summer School on Laser-Plasma Interactions, St. Andrews 1979

4. L.D. Landau and E.M. Lifshitz, Fluid Mechanics (Pergamon, London 1959)

5. A.G.M. Maaswinkel, K. Eidmann, and R. Sigel, Max-Planck-Gesellschaft zur Förderung der Wissenschaften e.V. Report No. PLF 10/1978.

6. Groupement de Recherches Coordonnées Interaction Laser-Matière, Rapport d'Activité 1979, Palaiseau.

7. F. Amiranoff, R. Fabbro, E. Fabre, C. Garban, J. Virmont, and M. Weinfeld, Phys. Rev. Lett. 43, 522 (1979)

8. J.E. Balmer and T.P. Donaldson, Phys. Rev. Lett. 39, 1084 (1977)

9. R.W.P. McWhirter, in "Plasma Diagnostic Techniques", ed. R.H. Huddlestone and S.L. Leonard (Academic Press, New York, 1965), Ch. 5.

10. P. Mulser and C. van Kessel, J. Phys. D 11, 1085 (1978)

11. G.P. Banfi, P.G. Gobbi, S. Morosi, and G.C. Reali, Appl. Phys. Lett. 37, 23 (1980)

12. R.P. Godwin, P. Sachsenmaier, and R. Sigel, Phys. Rev. Lett. 39, 1198 (1977)

13. J.J. Thomson, W.L. Kruer, A. Bruce Langdon, Claire Ellen Max, and W.C. Mead, Phys. Fluids 21, 707 (1978)

14. K.R. Manes, V.C. Rupert, J.M. Auerbach, P. Lee, and J.E. Swain, Phys. Rev. Lett. 39, 281 (1977)

15. M.D. Rosen, D.W. Phillion, V.C. Rupert, W.C. Mead, W.L. Kruer, J.J. Thomson, H.N. Kornblum, V.W. Slivinsky, G.J. Caporaso, M.J. Boyle, and K.G. Tirsell, Phys. Fluids 22, 2020 (1979)

16. R. Sigel, J. de Physique Colloque C6, 38, C6-35 1977

17. Lawrence Livermore Laboratory, Annual Report 1978, Sect. 3.1

NOTATION

A	normalized collision frequency $(\nu_{ei})_{N_{cr}} / \omega$
A_o	relative atomic mass
$\vec{B}$	magnetic induction
c	light velocity in vacuum
c_s	ion sound velocity
e	elementary charge
$\vec{E}$	electric field
f_{ib}	fractional inverse bremsstrahlung absorption
f_{ra}	fractional resonance absorption
I	intensity
I_{inc}	intensity of the incident beam
I_{abs}	absorbed intensity
$\vec{j}$	current density
k	vacuum wave number
k_B	Boltzmann constant
L	1. crystal length
	2. scale length at the critical density
m_e	electron mass
M_i	ion mass
n	1. refractive index
	2. variation of N
N_{cr}	critical density
N_e	electron density
N_i	ion density
N_o	equilibrium density
p_e	electron pressure
$P_{\omega, 2\omega}$	power at frequency $\omega, 2\omega$
R, R_{TOT}	reflectance; total reflectance
$R_{lin,exp}$	reflectance for a linear / exponential density profile
R_{ib}	inverse bremsstrahlung reflectance
$R^{S,P}_{DIFF}$	diffuse reflectance for a S, P-polarized beam
$R^{S,P}_{SPEC}$	specular reflectance for a S, P-polarized beam
t	time
T_e	electron temperature
T_i	ion temperature

u	normalized ion velocity v_i / c_s
v_e	electron velocity
v_i	ion velocity
x, y, z	cartesian coordinates
z	charge state
α, α_o, β	factors describing reflectance by inverse bremsstrahlung
ε_o	permittivity of the vacuum
ϑ_o	angle of incidence
λ	laser wavelength
$\ln \Lambda$	Coulomb logarithm
ν_{ei}	electron-ion collision frequency
ξ	self-similar parameter $x / c_s t$
$\tau, \Delta\tau$	time, time delay
ϕ	tilt angle of the critical density layer
Φ	potential
ω	angular frequency of the light wave
ω_{pe}	electron plasma frequency
$\approx$	approximately equal
$\sim$	proportional to
$>$	larger than
$\gtrsim$	larger or approximately equal
$<$	smaller than
$\lesssim$	smaller or approximately equal

ACKNOWLEDGEMENTS

Only when the results of a study have finally been written up does one fully appreciate the extent to which others have contributed to them. In particular, I am indebted to the following colleagues for their support:

R. Sigel, who familiarized me with laser-produced plasmas and showed continuous interest in supervising the progress of the work

S. Witkowski, who provided the opportunity of performing this work in his division;

K. Eidmann, who gave much helpful advice concerning the experiments; P. Mulser and especially Hans-Jörg Kull, who, in many discussions greatly furthered my understanding of the absorption process;

P. Sachsenmaier and E. Wanka, who provided excellent technical support during the experiments.

I highly appreciate the promptness with which I. Böckmann typed the manuscript despite other obligations. I also thank H. Brändlein and J. Pfister for providing the formulas and drawings.

Finally I wish to express my gratitude to Max-Planck-Gesellschaft and EURATOM for awarding a scholarship enabling me to conduct this study.

LEVENSLOOP

De schrijver van dit proefschrift werd geboren op 21 mei 1952 in Roosendaal. In deze plaats en in Nijmegen bezocht hij de lagere school. In Nijmegen legde hij in 1970 het eindexamen Gymnasium-Beta af aan het Canisiuscollege.

Hierna studeerde hij elektrotechniek aan de Technische Hogeschool Eindhoven. Tijdens de ingenieursfase van de studie deed hij in een stage van vier maanden voor het eerst ervaring op met lasersystemen; deze stage vond plaats aan het Institut für Plasmaphysik in Garching onder leiding van dr.ir. C.G.M. van Kessel.

Hij voerde zijn afstudeerwerk uit in de groep Direkte Omzetting onder leiding van Prof.dr. L.H.Th. Rietjens en dr. A. Veefkind. Na het behalen van het ingenieursexamen op 23 juni 1977 vertrok hij naar Garching. Het onderzoek daar in de Projektgruppe für Laserforschung onder leiding van dr. R. Sigel leidde tot dit proefschrift.

SAMENVATTING

"EXPERIMENTEEL ONDERZOEK VAN LINEAIRE MODE CONVERSIE IN LASERPLASMA'S"

Onderzocht zijn absorptiemechanismen in hete, dichte plasma's, die door laserbestraling van vlakke targets werden gemaakt. Daarbij stond het absorptiemechanisme van lineaire mode conversie centraal; dit proces treedt op in een inhomogeen plasma, indien de elektrische veldvektor in de invallende E.M.golf een komponent parallel aan de dichtheidsgradient heeft; hierdoor worden aan de kritische dichtheid (hier is $\omega_{pe} = \omega$) elektrostatische oscillaties veroorzaakt. Ook is absorptie van het laserlicht in het plasma door inverse bremsstrahlung onderzocht.

De absorptie werd bepaald uit de reflektie van het ingestraalde laserlicht aan het plasma. Hiertoe werden optische diagnostieken gebruikt; gemeten werd reflektie in 4π ruimtehoek (met een bol van Ulbricht) en reflektie in spiegelende (geometrische) richting. Door bovendien de polarisatie van het licht en de invalshoek tot het target te varieren konden de bijdragen van de absorptiemechanismen geisoleerd worden.

Als essentieel onderdeel van het onderzoek moet worden genoemd, dat het laserlicht door niet-lineaire kristallen in frekwentie verdubbeld en vervierVoudigd werd: hiermee werd voor het eerst de afhankelijkheid van absorptie in laserplasma's van de golflengte van de laser onderzocht. De parameters bij de experimenten waren: pulsduur 30 ps, intensiteit max. 10^{14} W/cm^2 en golflengten 1.06 µm, 0.53 µm en 0.26 µm.

Een vergelijking van de experimentele resultaten met de lineaire absorptiemechanismen toont, dat de absorptie goed wordt beschreven door lineaire mode conversie en inverse bremsstrahlung. Dit houdt in dat lasers met korte golflengten ($\lesssim$ 0.3 µm) en relatief lange pulsduur ($\gtrsim$ 1 ns) geschikte kandidaten zijn voor grote systemen in een laserfusie reaktor.

Stellingen

1. De absorptie van invallend laserlicht in een inhomogeen plasma door lineaire mode conversie kan worden opgevoerd tot 50%. Daar dit proces onafhankelijk is van de golflengte en intensiteit van de laserstraal, is het mogelijk het belangrijkste absorptiemechanisme voor een plasma in een laser-fusie reaktor.
   Dit proefschrift.

2. Absorptie van P-gepolariseerd licht in een inhomogeen isotroop plasma aan de kritische dichtheid wordt lineaire mode conversie en ook resonantie absorptie genoemd. De naam resonantie absorptie is reeds in gebruik in andere takken der natuurkunde ; bovendien is de benaming lineaire mode conversie nauwkeuriger en verdient derhalve de voorkeur.

3. In de berekening van resonantie absorptie aan een gerimpelde kritische dichtheid door Garban-Labaune et al. wordt ervan uitgegaan dat deze rimpels in het invalsvlak liggen. Indien de rimpels een stochastisch karakter hebben kunnen zij met gelijke waarschijnlijkheid loodrecht op het invalsvlak liggen ; de berekende resonantie absorptie door rimpeling is dan een faktor twee kleiner.
   C. Garban-Labaune et al., J.Physique Lettres 41, L463 (1980).

4. De correctie-term gevonden door Mulser/ Van Kessel voor de reflectiecoëfficiënt in een laserplasma met een lineair dichtheidsprofiel berust op een afbreekfout in de reeksontwikkeling voor η.
   P. Mulser en C.van Kessel, J.Phys.D. 11, 1085 (1978).

5. Bij het onderzoek van multiphoton-ionizatie (MPI) aan benzeen door middel van UV-laserbestraling is de duur van de laserpuls een essentiële parameter.

6. Bij het onderzoek naar kernfusie d.m.v. compressie van DT-pellets door laserbestraling dient meer aandacht te worden besteed aan het ontwikkelen van een laser met voldoende rendement (3 - 5%), hoge repetitie-frequentie ($\approx$ 1 Hz) en korte puls ($\lesssim$ 10 ns). Deze laser dient bij voorkeur een korte golflengte ($\approx$ 0.3 μm) te hebben.

7. De toepassing van het tokamak-principe in een fusie-reaktor is weinig waarschijnlijk ; dit volgt uit problemen samenhangend met de configuratie, en uit de lage netto vermogensdichtheid bij grote complexiteit en zeer intensief onderhoud van het systeem.
   Conclusie van K.H. Schmitter, Report IPP 4/170, juni 1978.

8. De stijgende kosten in de verschillende takken van het fundamentele onderzoek stellen een absolute grens aan de verdere uitbouw en beperken de vooruitgang in de afzonderlijke takken.

9. De graad van Diplomingenieur wordt in de toekomst in de Bondsrepubliek Duitsland zowel aan afgestudeerden van een Technische Universität als ook van een Fachhochschule toegekend. Door de toevoeging van de afkorting respektievelijk "Univ." en "FH" aan de titel wordt de beoogde gelijkstelling teniet gedaan en werkt de nieuwe titel inflatoir.
   Süddeutsche Zeitung, 17 juli 1980.

10. Het verlenen van tijdelijke contracten van 2 of 3 jaar aan jonge wetenschappelijke onderzoekers, hetgeen momenteel in de Bondsrepubliek Duitsland wordt toegepast, gaat uit van een irrealistische immobiliteit van de werknemer; bovendien kan het betwijfeld worden of de totale extra kosten verbonden aan deze contracten opwegen tegen de beoogde doorstroming.

11. Bij een meertalige promotiecommissie dienen de stellingen beschikbaar te zijn in de verschillende talen, zodat een algemene discussie hierover mogelijk is.
   Artikel 16 van het promotiereglement der Technische Hogeschool.
   Artikel 224 van het Academisch Statuut.

A.G.M. Maaswinkel

Eindhoven, 12 december 1980

Theses

1. The absorption of incident laser light in an inhomogeneous plasma by linear mode conversion can be increased to 50%. As this process is independent of the wavelength and intensity of the laser beam, it may well be the most important absorption mechanism for a plasma in a laser-fusion reactor.
   This dissertation.

2. Absorption of P-polarized light in an inhomogeneous isotropic plasma at the critical density is called linear mode conversion and also resonance absorption. The name resonance absorption is already being used in other fields of physics; in addition, the designation linear mode conversion is more exact and is therefore preferable.

3. In the computation of resonance absorption at a rippled critical density by Garban-Labaune et al. the assumption is made that these ripples are in the plane of incidence. If these ripples are of a stochastic nature they may be perpendicular to the plane of incidence with equal probability; the computed resonance absorption due to rippling is then a factor of two smaller.
   C. Garban-Labaune et al., J.Physique Lettres 41, L463 (1980).

4. The correction term found by Mulser/ Van Kessel for the reflection coefficient in a laser-produced plasma with a linear density profile results from a truncation error in the series expansion for η.
   P. Mulser and C.van Kessel, J.Phys.D. 11, 1085 (1978).

5. In the investigation of multi-photon ionization (MPI) in benzene by UV laser irradiation the pulse length of the laser is an essential parameter.

6. In research into thermonuclear fusion by compression of DT pellets by laser irradiation more attention should be paid to the development of a laser with sufficient efficiency (3 to 5%), high repetition rate ($\approx$ 1 Hz) and short pulse length ($\lesssim$ 10 ns). This laser should preferably have a short wavelength ($\simeq$ 0.3 μm).

7. The applicability of the tokamak principle in a fusion reactor is not very probable; this is due to problems relating to the configuration, and to the small net power density in conjunction with the high complexity of the system and the intensive maintenance required.
   Conclusion from K.H. Schmitter, Report IPP 4/170, June 1978.

8. Rising costs in the different fields of basic research set an absolute limit to further outlay and restrict progress in them.

9. In the Federal Republic of Germany the degree of "Diplomingenieur" will be awarded in future to graduates both from a Technische Universität and from a Fachhochschule. By addition of the abbreviations "Univ." and "FH", respectively, to the title the equality intended is undone and the new title becomes inflationary.
   Süddeutsche Zeitung, July 17, 1980.

10. The award of temporary contracts for 2 or 3 years to young scientists, which is being practised in the Federal Republic of Germany at the moment, originates from an unrealistic immobility of the employees; moreover, it is doubtful whether the renewal intended is worth the extra costs involved.

11. With a polyglot board of examiners the theses should be available in the different languages to allow general discussion on them.
    Article 16 of the "Promotiereglement der Technische Hogeschool".
    Article 224 of the "Academisch Statuut".

A.G.M. Maaswinkel

Eindhoven, December 12, 1980